Document ID
1569690, (1.0 Approved)
Reg no

Security class
Public
Document type
Memo

Page
1(59)

Author
2017-04-01 Jordi Bruno, Lara Duro, Olga Riba
Quality assurance
2017-05-08 Klas Källström (Approved)

Supplementary information on colloid interactions in SFR

Table of contents

1Introduction

Low and intermediate level waste from the operation of Swedish NPPs is stored in the SFR repository. The facility is located in the bedrock at a depth of approximately 50 m and has been in operation for 20 years. In order to host decommissioning waste and additional operational waste, the storage volume of the SFR repository must be extended with approximately 140 000 m^3. To do this, the SFR extension project (PSU) has submitted a license application to extend SFR by December 2014 and the superior aim of having the extended facility in operation by year 2028.
Recently, SSM has started to request to SKB additional information (*kompletteringar)* regarding a number of issues, among them SSM has requested additional information on the potential effects of eigen and cementitious colloids on the solubility and mobility of Pu and Am in the various parts of the repository, including their interaction with the bentonite from the Silo.
Specifically, the following points have been requested by SSM to be complemented with additional information:

1. An estimate of the maximum concentration (in moles per litre water) of Pu and Am in different parts of the repository, based on inventory of Pu and Am and amounts of pore water and free water in each repository.
2. A comparison of the possible concentrations of Pu and Am (Obtained from point 1) with their respective solubilities in the repository environment i.e. taking into account expected redox and pH conditions and the concentrations of complexing agents.
3. Recognition of the risk of formation of eigencolloids (eng. Intrinsic Colloids) of Pu and Am and assessment of colloidal stability in the repository parts where solubility is exceeded. These accounts should include theoretical analysis and experimental results showing impact of two conflicting factors, high pH and high concentration of divalent cations from the alkaline earth metals (mainly Ca^{2+}). These factors have contrary effects on colloidal stability.
4. If necessary, discuss the possibility of bentonite in the silo filtering eigencolloids consisting of Pu and Am.
5. Quantification of the ratio of sorption of radionuclides on the surface of cement colloids to sorption of radionuclides on the surfaces of cement matrix in the repository environment
6. Stability of formed cement colloids in the repository environment

1.1 Objective

The main objective is to assist SKB in preparing a well-founded and thorough response to these demands.

2 Methodology

In order to tackle the issues Amphos 21 has performed the following actions:

1. Calculation of the maximum Pu and Am inventories in the various parts of SFR by using the data previously provided by the PSU project team for the previous sorption reduction factor calculations.
2. Re-calculation of the maximum Pu and Am solubilities in the various parts of the repository taking into consideration organic ligands complexation, as requested by SSM. The calculations will be performed by using the Thermochimie data base which is the most updated and traceable data base for this purpose.
3. Assessment of the stability of eigencolloids of Pu and Am under the repository conditions, including a thorough discussion of the effects of alkalinity vs Ca(II) concentration on colloidal stability.
4. Assessment and quantification of the potential partition of eigencolloids in the cement surface.
5. Assessment of the stability and transport of the eigencolloids in the bentonite barrier of the Silo.
6. Assessment of the stability of cementitious colloids under repository conditions, based on an extension and update of the information already included in the Waste Process Report (SKB 2014b)

3 Results

3.1 Calculation of the maximum Pu and Am inventories in the various parts of SFR.

The inventory for Am and Pu in the various parts of the repository is given as best estimate in the Initial State Report for the Safety Assessment PSU, SKB TR-14-02 (SKB 2014a). This inventory is shown (in Becquerels) in Table 3-1.

Table 3-1. Inventory of activity (in Becquerels) for Am and Pu (from SKB TR-14-02). The value shown in the table corresponds to the sum of activity reported for each isotope. The value for the BTF vault is an average of 1BTF and 2BTF.

Metal/RN (Becquerel)	Silo vault	1BMA vault	2BMA vault	BTF vault
Am	$2.32 \cdot 10^{13}$	$2.93 \cdot 10^{10}$	$4.20 \cdot 10^{10}$	$4.02 \cdot 10^{9}$
Pu	$4.21 \cdot 10^{11}$	$3.82 \cdot 10^{10}$	$2.26 \cdot 10^{11}$	$6.86 \cdot 10^{9}$

The activity in Becquerels for each specific isotope where converted to moles by taking into account the corresponding half-life value for each individual isotope. The value in moles was then converted into concentrations (moles/litre) by taking into account the void volume and the porosity of the materials for each section of the repository, as reported in SKB TR-14-02 and summarized in Table 3-2.

Table 3-2. Void + pore volume (in m^3) for the different parts of the SFR repository used in the calculations (from SKB TR-14-02). The value for the BTF vault is an average of 1BTF and 2BTF.

	Silo vault	1BMA vault	2BMA vault	BTF vault
Void + pore volume (m^3)	$7.21 \cdot 10^{3}$	$4.48 \cdot 10^{3}$	$8.63 \cdot 10^{3}$	$6.65 \cdot 10^{3}$

The final concentrations used in the calculations reported in present work are summarized in Table 3-3. When concentrations for more than one isotope of the same radionuclide were provided in the inventory, the final concentration shown in the table corresponds to the sum of all the isotopes available. For example: in the case of Plutonium, the concentration shown in Table 3-3 corresponds to the sum of concentrations for ^{238}Pu, ^{239}Pu, ^{240}Pu, ^{241}Pu and ^{242}Pu calculated from the original inventory.

Table 3-3. Concentrations of metals and radionuclides used in the calculations in present work.

Metal/RN ($mol.dm^{-3}$)	Silo vault	1BMA vault	2BMA vault	BTF vault
Am	$1.05 \cdot 10^{-7}$	$2.38 \cdot 10^{-10}$	$1.99 \cdot 10^{-10}$	$2.20 \cdot 10^{-11}$
Pu	$6.54 \cdot 10^{-9}$	$1.70 \cdot 10^{-9}$	$2.18 \cdot 10^{-9}$	$1.32 \cdot 10^{-10}$

3.1.1 Porewater composition

In order to proceed to the following step of the assessment, this is the calculation of the solubility limits, we need to quantify the chemical evolution of the cement porewater. The alkaline environment imposed by cement and concrete materials will evolve with time as those materials degrade. The different cement degradation stages will lead to different cement porewater composition, with different OH^- concentration, different pH and calcium concentrations. Those changes will affect the speciation of the analysed radionuclides, as well as the potential stability of colloids.

The typical mineral evolution and the corresponding pH evolution for cement is reported in Cronstrand (2014). Initially, cement porewater is characterised by high OH^- and high Na and K concentrations, due to the dissolution of alkali oxides by pH=13.06 . As cement degrades, OH^- concentration decreases and portlandite controls the pH at ≈12.6. As cement degradation proceeds, OH^- concentration decreases during the decalcification of CSH phases in the interval 12-11. After CSH dissolution continues, pH drops to levels below 10, buffered by remaining cement specific minerals or precipitated hydroxides.

In order to capture the essence of this evolution, four different cement porewater compositions have been selected to perform the solubility and speciation calculations:

- **Porewater "A" (pH=13.06):** Reported in Cronstrand (2014). Corresponds to the initial composition of cement porewater assumed to be a mixture between pure concrete porewater and the temperate-preglacial water infiltrating in SFR, scaled to the fractional content of cement and concrete in the vaults.

- **Porewater "B" (pH=12.60):** Reported in SKB (2008). Corresponds to a leached cement porewater, representing a degradation state where highly soluble alkali hydroxides have been leached out and the pH is buffered by calcium hydroxide (portlandite).

- **Porewater "C" (pH=11.60):** Water composition calculated as a result of the dissolution of SFR concrete by fresh groundwater. At this stage, CSH dissolution dominates the porewater chemistry.

- **Porewater "D" (pH=9.66):** Water composition calculated as a result of the dissolution of SFR concrete by fresh groundwater. It corresponds to an advanced degradation state with no CSH phases present any longer.

The chemical compositions of the four different cement porewaters studied are summarized in .

Table *3-4*.

Table *3-4*. Composition of the cement porewaters used in present work to perform speciation calculations.

Metal (M)	Porewater A pH=13.06	Porewater B pH=12.60	Porewater C pH=11.60	Porewater D pH=9.66
OH^-	0.114	0.04	$3.9\cdot10^{-3}$	$4{,}57\cdot10^{-5}$
Ca	$1.48\cdot10^{-3}$	$2.00\cdot10^{-2}$	$2.59\cdot10^{-3}$	$4.57\cdot10^{-5}$
Al	$9.66\cdot10^{-6}$	$2.00\cdot10^{-6}$	-	-
C (IV)	$1.53\cdot10^{-3}$	-	$9.81\cdot10^{-6}$	$8.79\cdot10^{-4}$
Cl	$1.61\cdot10^{-3}$	$2.00\cdot10^{-3}$	$5.36\cdot10^{-3}$	$5.36\cdot10^{-3}$
K	$1.12\cdot10^{-1}$	$1.00\cdot10^{-4}$	$1.28\cdot10^{-4}$	$1.28\cdot10^{-4}$
Mg	$1.48\cdot10^{-4}$	-	$1.23\cdot10^{-8}$	$3.01\cdot10^{-5}$
Na	$5.01\cdot10^{-2}$	$3.00\cdot10^{-3}$	$7.83\cdot10^{-3}$	$7.83\cdot10^{-3}$
S (VI)	$3.53\cdot10^{-4}$	$2.00\cdot10^{-5}$	$1.00\cdot10^{-3}$	$5.21\cdot10^{-4}$
Si	$8.38\cdot10^{-5}$	$3.00\cdot10^{-6}$	$5.63\cdot10^{-4}$	$2.00\cdot10^{-4}$

The calculations have been performed under two different redox conditions covering the range of the redox potentials calculated as a function of the active redox couple controlling the cementitious system (Duro et al. 2012).

1) Eh = 0 V, being the upper redox limit

2) Eh determined by the redox couple magnetite/hematite at the different pH's given by the degradation of cementitious materials.

3.1.2 Organic ligands

The operating waste in the repository contains different organic substances, whose composition and volumes may vary considerably. Knowledge of radionuclide complexation with those organic ligands is important because:

- complexation of a radionuclide increases its solubility, and thus its mobility; and
- adsorption of metal ions on solid surfaces (such as cement) is affected by organic complex formation, normally decreasing the extent of sorption.

The main organic ligands of interest within this work are Isosaccharinate (ISA) and Ethylenediaminetetraacetate (EDTA) (Figure 3-1). Notice that, in the formulas, the Isosaccharinate ion will be written as "$ISAH_2^-$, where "H_2" refers to the hydrogens of the secondary alcohols in the molecule.

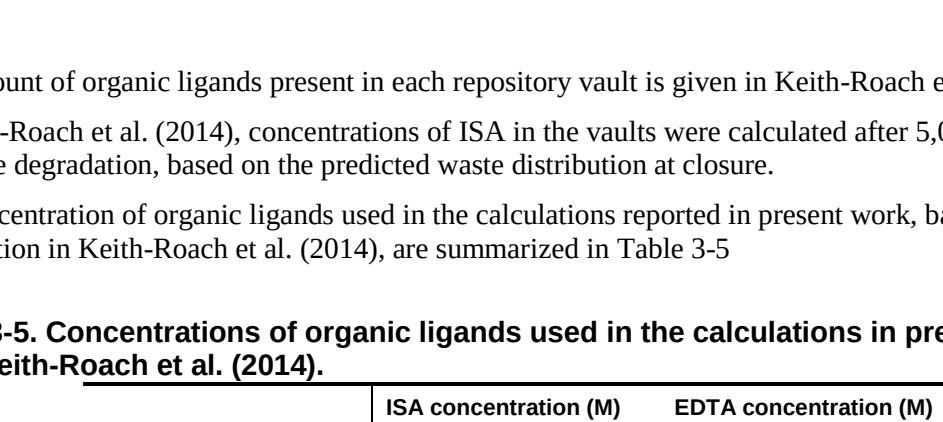

ISA EDTA

Figure 3-1 Isosaccharinate and EDTA chemical structures.

The amount of organic ligands present in each repository vault is given in Keith-Roach et al. (2014).

In Keith-Roach et al. (2014), concentrations of ISA in the vaults were calculated after 5,000 years of cellulose degradation, based on the predicted waste distribution at closure.

The concentration of organic ligands used in the calculations reported in present work, based on the information in Keith-Roach et al. (2014), are summarized in Table 3-5

Table 3-5. Concentrations of organic ligands used in the calculations in present work, from Keith-Roach et al. (2014).

	ISA concentration (M) Sorption[(a)]	EDTA concentration (M)
Silo vault	$3.8 \cdot 10^{-5}$	$5.2 \cdot 10^{-7}$
1BMA vault	$2.9 \cdot 10^{-4}$	$3.8 \cdot 10^{-6}$
2BMA vault	$2.6 \cdot 10^{-4}$	[(b)]
BTF vault	$4.5 \cdot 10^{-6}$	$1.3 \cdot 10^{-6}$

(a) ISA concentrations as reported in Keith-Roach et al. (2014). The concentrations were calculated taking into account the amount of ISA sorbed onto hydrated cement.
(b) The concentration of EDTA in the 2BMA vault is considered not significant in Keith-Roach et al. (2014).

3.2 Re-calculation of the maximum Pu and Am solubilities in the various parts of the repository taking into consideration organic ligands complexation.

The calculation of the maximum Pu and Am solubilities in the various parts of the repository has been done by taking into consideration organic ligands complexation. The calculations are performed with PhreeqC code version 3.3.5 (Parkhurst and Appelo 2013) by using the Thermochimie v9b0 data base (Giffaut et al. 2014) which is the most updated and traceable data base for this purpose.
Speciation and solubility calculations have been carried out using the porewaters, the organic ligands inventories and the radionuclide inventories described in the previous section for each part of the repository. The results are described in Appendix A.
In order to assess the impact of colloids in the plutonium and americium solubility, calculations considering precipitation of the colloidal phases: PuO_2(coll,hyd), $Pu(OH)_3$(coll) and $Am(OH)_3$(coll) and the non-colloidal phases: $Pu(OH)_4$(am), $Pu(OH)_3$(cr) and $Am(OH)_3$(am) have been carried out. The Pu(IV) colloidal phase PuO_2(coll, hyd) is included in Thermochimie v9b0 data base with an associated constant that differs one order of magnitude respect to $Pu(OH)_4$(am) (see Table 3-6), however, there are no colloidal phases associated to Pu(III) and Am(III) hydroxides currently included in ThermoChimie. For this reason, the reactions presented in Table 3-6 corresponding to $Pu(OH)_3$(coll) and $Am(OH)_3$(coll) have also been included in the calculations. The same difference of solubility constants between the colloidal and the non-colloidal phases for Pu(IV) have been considered for the Pu(III) and Am(III) colloidal phases.

Table *3-6*. Formation reactions with the associated equilibrium constants used to assess the impact of Pu and Am colloids.

Reaction	Log K
$Pu^{4+} + 4H_2O = Pu(OH)_4(am) + 4H^+$	0.8
$Pu^{4+} + 2H_2O = PuO_2(coll,hyd) + 4H^+$	-0.2
$Pu^{3+} + 3H_2O = Pu(OH)_3(cr) + 3H^+$	-15.8
$Pu^{3+} + 3H_2O = Pu(OH)_3(coll) + 3H^+$	**-16.8***
$Am^{3+} + 3H_2O = Am(OH)_3(am) + 3H^+$	-16.9
$Am^{3+} + 3H_2O = Am(OH)_3(coll) + 3H^+$	**-17.9***

* *These phases are not included in ThermoChime v9b0*

Here, we will present the most relevant cases, which concern the solubility of Am and Pu in the Silo, where the inventory of both nuclides is larger.

Two types of calculations are presented, in the first case we calculate the potential saturation of colloidal Am and Pu phases assuming the calculated concentrations from the actual inventories in the Silo as given in Table 3-3. In a second kind of calculations we assume a larger input of Am and Pu, 10^{-5} mol dm^{-3} and we let the system equilibrate with colloidal Am and Pu phases.

For each calculation type, two redox conditions are assumed: a) by considering an upper redox limit Eh=0 mV and b) by assuming redox buffering by the anaerobic reduction of iron, according to SKB TR-12-12.

Firstly, we will discuss the effects of organics on the results of the calculations of Am and Pu solubilities at Eh=0, assuming the initial inventory calculations as given in Table 3-7.

Table *3-7*. Radionuclide speciation and equilibrium concentration for Am and Pu in the SILO. $[ISA]_{aq}=3.8\cdot10^{-5}$ M (considering ISA sorption) and $[EDTA]_T=5.2\cdot10^{-7}$ M. Only species accounting for ≥10% of the dissolved radionuclide speciation are shown.

Porewater	A	B	C	D

pH	13.06	12.60	11.60	9.66
pe	0	0	0	0
$[Ca]_T$ (M)	$1.49 \cdot 10^{-3}$	$2.00 \cdot 10^{-2}$	$2.59 \cdot 10^{-3}$	$4.57 \cdot 10^{-5}$
Am $[Am]_T = 1.1 \cdot 10^{-7}$	**$Am(OH)_3$(coll)** $[Am]_{aq} = 1.4 \cdot 10^{-8}$	**$Am(OH)_3$(coll)** $[Am]_{aq} = 9.8 \cdot 10^{-9}$	**$Am(OH)_3$(coll)** $[Am]_{aq} = 1.6 \cdot 10^{-8}$	**No precipitation** $[Am]_{aq} = 1.1 \cdot 10^{-7}$
	$Am(OH)_3(ISAH_2)^-$ (63.1%) $Am(OH)_3$ (34.7%)	$Am(OH)_3$ (50.3%) $Am(OH)_3(ISAH_2)^-$ (45.6%)	$Am(OH)_3(ISAH_2)^-$ (56.3%) $Am(OH)_3$ (32.1%) $Am(OH)_2^+$ (11.5%)	$Am(EDTA)^-$ (53.8%) $Am(CO_3)^+$ (30.4%)
	$Am(OH)_3$(am) $[Am]_{aq} = 1.4 \cdot 10^{-9}$	**$Am(OH)_3$(am)** $[Am]_{aq} = 9.8 \cdot 10^{-10}$	**$Am(OH)_3$(am)** $[Am]_{aq} = 1.6 \cdot 10^{-9}$	**No precipitation** $[Am]_{aq} = 1.1 \cdot 10^{-7}$
	$Am(OH)_3(ISAH_2)^-$ (63.0%) $Am(OH)_3$ (34.7%)	$Am(OH)_3$ (50.3%) $Am(OH)_3(ISAH_2)^-$ (45.6%)	$Am(OH)_3(ISAH_2)^-$ (56.3%) $Am(OH)_3$ (32.1%) $Am(OH)_2^+$ (11.5%)	$Am(EDTA)^-$ (53.8%) $Am(CO_3)^+$ (30.4%)
Pu $[Pu]_T = 6.5 \cdot 10^{-9}$ ***PuO_2(coll, hyd) is never oversaturated***	**$Pu(OH)_4$(am)** $[Pu]_{aq} = 3.6 \cdot 10^{-9}$	**$Pu(OH)_4$(am)** $[Pu]_{aq} = 1.6 \cdot 10^{-9}$	**$Pu(OH)_4$(am)** $[Pu]_{aq} = 3.1 \cdot 10^{-9}$	**$Pu(OH)_4$(am)** $[Pu]_{aq} = 3.5 \cdot 10^{-9}$
	$Pu(OH)_4(ISAH_2)_2^{2-}$ (47.5%) $Pu(OH)_4(ISAH_2)^-$ (39.0%) $Pu(OH)_4$ (13.5%)	$Pu(OH)_4(ISAH_2)^-$ (44.7%) $Pu(OH)_4$ (31.1%) $Pu(OH)_4(ISAH_2)_2^{2-}$ (24.2%)	$Pu(OH)_4(ISAH_2)^-$ (44.4%) $Pu(OH)_4(ISAH_2)_2^{2-}$ (39.6%) $Pu(OH)_4$ (16.0%)	$Pu(OH)_4(ISAH_2)^-$ (43.5%) $Pu(OH)_4(ISAH_2)_2^{2-}$ (39.9%) $Pu(OH)_4$ (14.4%)

Table 3-8. Radionuclide speciation and equilibrium concentration for Am and Pu in the SILO in absence of organics. Only species with ≥10% are shown.

Porewater	A	B	C	D
pH	13.06	12.60	11.60	9.66
pe	0	0	0	0
$[Ca]_T$ (M)	$1.49 \cdot 10^{-3}$	$2.00 \cdot 10^{-2}$	$2.59 \cdot 10^{-3}$	$4.57 \cdot 10^{-5}$
Am $[Am]_T = 1.1 \cdot 10^{-7}$	**$Am(OH)_3$(coll)** $[Am]_{aq} = 5.2 \cdot 10^{-9}$	**$Am(OH)_3$(coll)** $[Am]_{aq} = 5.4 \cdot 10^{-9}$	**$Am(OH)_3$(coll)** $[Am]_{aq} = 6.8 \cdot 10^{-9}$	**No precipitation** $[Am]_{aq} = 1.1 \cdot 10^{-7}$
	$Am(OH)_3$ (93.9%)	$Am(OH)_3$ (92.5%)	$Am(OH)_3$ (73.4%) $Am(OH)_2^+$ (26.4%)	$Am(CO_3)_2^-$ (66.5%) $Am(OH)_2^+$ (16.8%) $Am(CO_3)^+$ (10.3%)
	$Am(OH)_3$(am) $[Am]_{aq} = 5.2 \cdot 10^{-10}$	**$Am(OH)_3$(am)** $[Am]_{aq} = 5.4 \cdot 10^{-10}$	**$Am(OH)_3$(am)** $[Am]_{aq} = 6.8 \cdot 10^{-10}$	**$Am(OH)_3$(am)** $[Am]_{aq} = 9.0 \cdot 10^{-8}$
	$Am(OH)_3$ (93.9%)	$Am(OH)_3$ (92.5%)	$Am(OH)_3$ (73.4%) $Am(OH)_2^+$ (26.4%)	$Am(CO_3)_2^-$ (66.5%) $Am(OH)_2^+$ (16.8%) $Am(CO_3)^+$ (10.3%)
Pu $[Pu]_T = 6.5 \cdot 10^{-9}$	**PuO_2(coll, hyd)** $[Pu]_{aq} = 4.8 \cdot 10^{-9}$	**PuO_2(coll, hyd)** $[Pu]_{aq} = 4.9 \cdot 10^{-9}$	**PuO_2(coll, hyd)** $[Pu]_{aq} = 5.0 \cdot 10^{-9}$	**PuO_2(coll, hyd)** $[Pu]_{aq} = 5.1 \cdot 10^{-9}$
	$Pu(OH)_4$ (100%)	$Pu(OH)_4$ (100%)	$Pu(OH)_4$ (100%)	$Pu(OH)_4$ (97.9%)
	$Pu(OH)_4$(am) $[Pu]_{aq} = 4.8 \cdot 10^{-10}$	**$Pu(OH)_4$(am)** $[Pu]_{aq} = 4.9 \cdot 10^{-10}$	**$Pu(OH)_4$(am)** $[Pu]_{aq} = 5.0 \cdot 10^{-10}$	**$Pu(OH)_4$(am)** $[Pu]_{aq} = 5.1 \cdot 10^{-10}$
	$Pu(OH)_4$ (100%)	$Pu(OH)_4$ (100%)	$Pu(OH)_4$ (100%)	$Pu(OH)_4$ (97.9%)

By comparing the results in Table 3-7 and

Table 3-8 it is clear that organic complexation has a strong effect on the solubility of Am and Pu phases and that in the presence of ISA and EDTA the colloidal Pu(IV) phase is not saturated and therefore the Pu concentrations are controlled by the inventory content in the Silo. The same applies for Am in contact with altered cement at pH=9.66, as aqueous Am(III) carbonate complexes become predominant.
A similar set of calculations was performed by assuming that the redox potential was controlled by the anaerobic reduction of iron and the subsequent equilibrium with magnetite (SKB TR-12-12). This set of calculations is shown in Table 3-9 and Table 3-10.

Table 3-9. Radionuclide speciation and equilibrium concentration for Am and Pu in the SILO. $[ISA]_{aq}=3.8\cdot10^{-5}$ M (considering ISA sorption) and $[EDTA]_T=5.23\cdot10^{-7}$ M. Only species accounting for ≥10% of the dissolved radionuclide speciation are shown.

Porewater	A	B	C	D

pH	13.06	12.60	11.60	9.66
pe	-11.79	-11.34	-10.35	-8.45
$[Ca]_T$ (M)	$1.49 \cdot 10^{-3}$	$2.00 \cdot 10^{-2}$	$2.59 \cdot 10^{-3}$	$4.57 \cdot 10^{-5}$
Am $[Am]_T = 1.1 \cdot 10^{-7}$	**$Am(OH)_3$(coll)** $[Am]_{aq} = 1.4 \cdot 10^{-8}$	**$Am(OH)_3$(coll)** $[Am]_{aq} = 9.8 \cdot 10^{-9}$	**$Am(OH)_3$(coll)** $[Am]_{aq} = 1.6 \cdot 10^{-8}$	**No precipitation** $[Am]_{aq} = 1.1 \cdot 10^{-7}$
	$Am(OH)_3(ISAH_2)^-$ (63.1%) $Am(OH)_3$ (34.7%)	$Am(OH)_3$ (50.3%) $Am(OH)_3(ISAH_2)^-$ (45.6%)	$Am(OH)_3(ISAH_2)^-$ (56.3%) $Am(OH)_3$ (32.1%) $Am(OH)_2^+$ (11.5%)	$Am((EDTA)^-$ (53.6%) $Am(CO_3)_2^-$ (30.5%)
	$Am(OH)_3$(am) $[Am]_{aq} = 1.4 \cdot 10^{-9}$	**$Am(OH)_3$(am)** $[Am]_{aq} = 9.8 \cdot 10^{-10}$	**$Am(OH)_3$(am)** $[Am]_{aq} = 1.6 \cdot 10^{-9}$	**No precipitation** $[Am]_{aq} = 1.1 \cdot 10^{-7}$
	$Am(OH)_3(ISAH_2)^-$ (63.1%) $Am(OH)_3$ (34.7%)	$Am(OH)_3$ (50.3%) $Am(OH)_3(ISAH_2)^-$ (45.6%)	$Am(OH)_3(ISAH_2)^-$ (56.3%) $Am(OH)_3$ (32.1%) $Am(OH)_2^+$ (11.5%)	$Am(EDTA)^-$ (53.6%) $Am(CO_3)_2^-$ (30.5%)
Pu $[Pu]_T = 6.5 \cdot 10^{-9}$ ***$Pu(OH)_3$(coll) is never oversaturated***	**$Pu(OH)_3$(cr)** $[Pu]_{aq} = 5.7 \cdot 10^{-9}$	**$Pu(OH)_3$(cr)** $[Pu]_{aq} = 2.7 \cdot 10^{-9}$	**$Pu(OH)_3$(cr)** $[Pu]_{aq} = 4.8 \cdot 10^{-9}$	**No precipitation** $[Pu]_{aq} = 6.5 \cdot 10^{-9}$
	$Pu(OH)_4(ISAH_2)_2^{2-}$ (45.0%) $Pu(OH)_4(ISAH_2)^-$ (36.9%) $Pu(OH)_4$ (12.8%)	$Pu(OH)_4(ISAH_2)^-$ (39.5%) $Pu(OH)_4$ (27.5%) $Pu(OH)_4(ISAH_2)_2^{2-}$ (21.3%) $Pu(OH)_3$ (11.7%)	$Pu(OH)_4(ISAH_2)^-$ (41.5%) $Pu(OH)_4(ISAH_2)_2^{2-}$ (37%) $Pu(OH)_4$ (14.9%)	$Pu(EDTA)^-$ (60.0%) $Pu(CO_3)_3^{3-}$ (18.5%)

The calculations in reducing conditions assuming no organics present are shown in the following Table 3-10.

Table 3-10. Radionuclide speciation and equilibrium concentration for Am and Pu in the SILO in absence of organics. Only species with ≥10% are shown.

Porewater	**A**	**B**	**C**	**D**

pH	13.06	12.60	11.60	9.66
pe	-11.79	-11.34	-10.35	-8.45
$[Ca]_T$ (M)	$1.49 \cdot 10^{-3}$	$2.00 \cdot 10^{-2}$	$2.59 \cdot 10^{-3}$	$4.57 \cdot 10^{-5}$
Am $[Am]_T = 1.1 \cdot 10^{-7}$	**$Am(OH)_3$(coll)** $[Am]_{aq} = 5.2 \cdot 10^{-9}$ $Am(OH)_3$ (93.9%)	**$Am(OH)_3$(coll)** $[Am]_{aq} = 5.4 \cdot 10^{-9}$ $Am(OH)_3$ (92.5%)	**$Am(OH)_3$(coll)** $[Am]_{aq} = 6.8 \cdot 10^{-9}$ $Am(OH)_3$ (73.4%) $Am(OH)_2^+$ (26.4%)	**No precipitation** $[Am]_{aq} = 1.1 \cdot 10^{-7}$ $Am(CO_3)_2^-$ (66.5%) $Am(OH)_2^+$ (16.8%) $Am(CO_3)^+$ (10.3%)
	$Am(OH)_3$(am) $[Am]_{aq} = 5.2 \cdot 10^{-10}$ $Am(OH)_3$ (93.9%)	**$Am(OH)_3$(am)** $[Am]_{aq} = 5.4 \cdot 10^{-10}$ $Am(OH)_3$ (92.5%)	**$Am(OH)_3$(am)** $[Am]_{aq} = 6.8 \cdot 10^{-10}$ $Am(OH)_3$ (73.4%) $Am(OH)_2^+$ (26.4%)	**$Am(OH)_3$(am)** $[Am]_{aq} = 9.0 \cdot 10^{-8}$ $Am(CO_3)_2^-$ (66.5%) $Am(OH)_2^+$ (16.8%) $Am(CO_3)^+$ (10.3%)
Pu $[Pu]_T = 6.5 \cdot 10^{-9}$ ***$Pu(OH)_3$(coll) is never oversaturated***	**$Pu(OH)_3$(cr)** $[Pu]_{aq} = 1.03 \cdot 10^{-9}$ $Pu(OH)_4$ (70.5%) $Pu(OH)_3$ (29.5%)	**$Pu(OH)_3$(cr)** $[Pu]_{aq} = 1.04 \cdot 10^{-9}$ $Pu(OH)_4$ (70.1%) $Pu(OH)_3$ (29.9%)	**$Pu(OH)_3$(cr)** $[Pu]_{aq} = 1.04 \cdot 10^{-9}$ $Pu(OH)_4$ (69.4%) $Pu(OH)_3$ (30.3%)	**No precipitation** $[Pu]_{aq} = 6.5 \cdot 10^{-9}$ $Pu(CO_3)_3^{3-}$ (59.0%) $Pu(CO_3)_2^-$ (29.4%)

The graphical representation of the main results for the inventory case is given in the following Figure 3-2 and Figure 3-3.

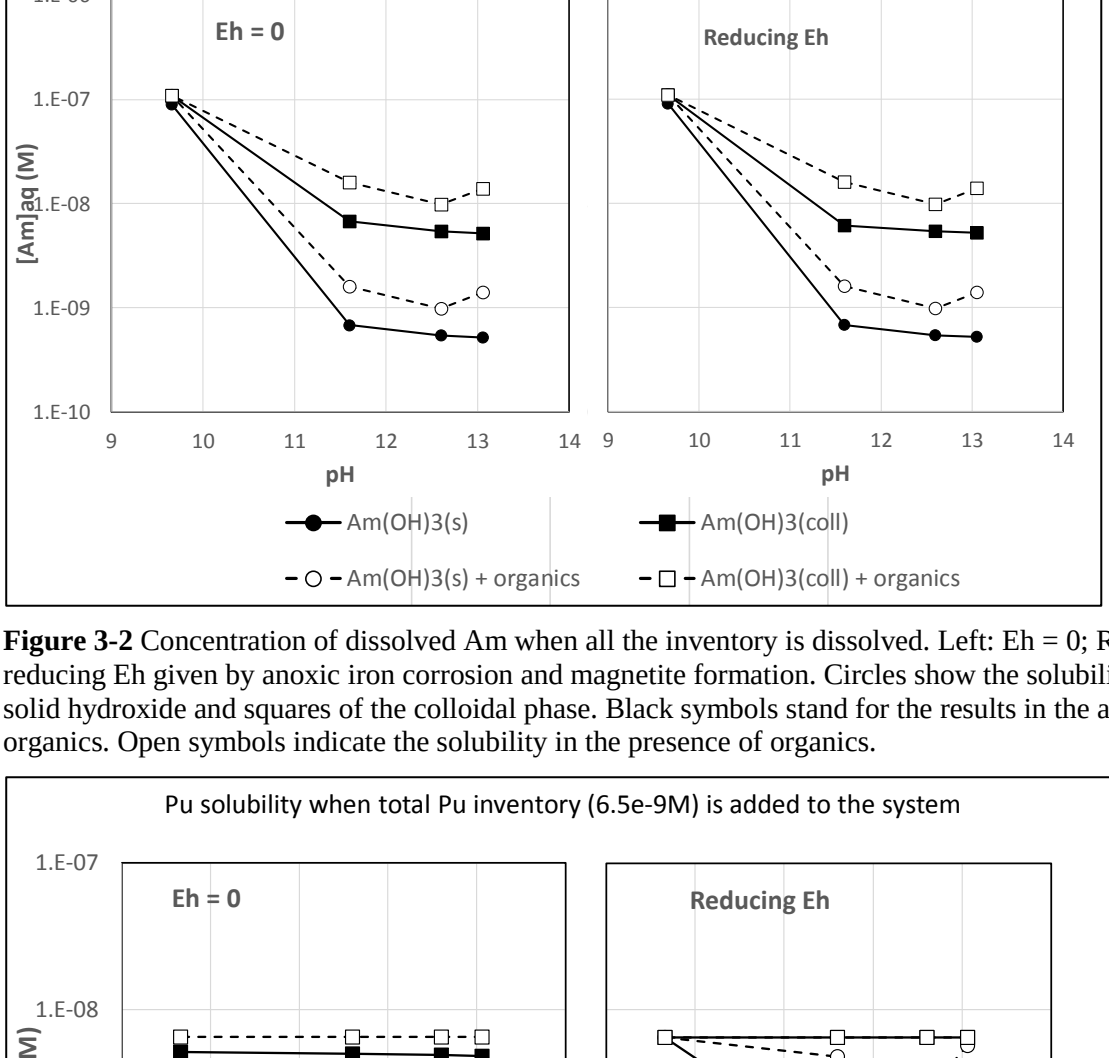

Figure 3-2 Concentration of dissolved Am when all the inventory is dissolved. Left: Eh = 0; Right: reducing Eh given by anoxic iron corrosion and magnetite formation. Circles show the solubility of the solid hydroxide and squares of the colloidal phase. Black symbols stand for the results in the absence of organics. Open symbols indicate the solubility in the presence of organics.

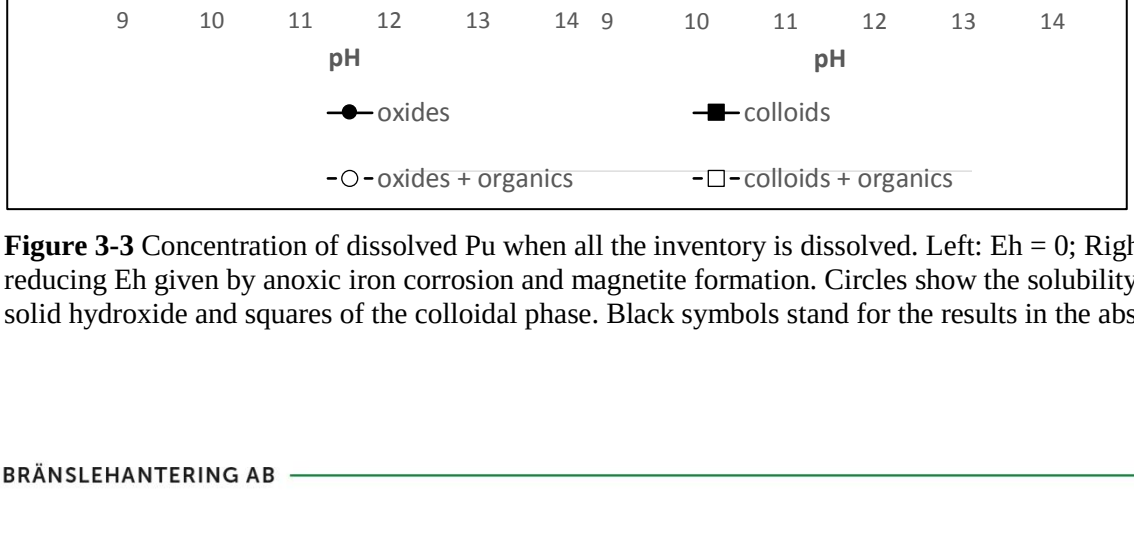

Figure 3-3 Concentration of dissolved Pu when all the inventory is dissolved. Left: Eh = 0; Right: reducing Eh given by anoxic iron corrosion and magnetite formation. Circles show the solubility of the solid hydroxide and squares of the colloidal phase. Black symbols stand for the results in the absence of

organics. Open symbols indicate the solubility in the presence of organics. Pu(IV) solids and Pu(III) are respectively considered for Eh = 0 and reducing Eh.

As expected, there are no changes in the solubility and speciation of Am as the redox potential becomes more reducing. However, for Pu there are some changes as the predominant solid phases are Pu(III) oxides and hydroxides. Under reducing conditions, the expected Pu concentrations are somewhat higher than at Eh=0, but still at the same order of magnitude.
In all cases, if we assume the formation of Pu colloidal phases the concentration of Pu is not solubility limited and it is controlled by the inventory content. This is not the case for Am, where as far as the cement degradation has not proceeded to the extinction of the CSH phases, the americium concentration is solubility controlled, even in the case when the formation of colloidal $Am(OH)_3$ is assumed. If degradation proceeds to pH=9.66, then Am(III) carbonate complexes are sufficiently strong to solubilize the totality of the Am content in the Silo at least up to 10^{-7} mol·dm^3 level.

In order to check at which inventory concentrations the Am and Pu content becomes solubility controlled, either by the formation of colloidal hydroxides, we have performed some calculations in which we have input an Am and Pu much larger than expected, at the 10^{-5} mol·dm^{-3} level. The calculations have been performed following the same hypothesis as in the previous cases.
The outcome of the calculations is given in the following Tables and Figures. The calculations are first performed assuming an upper limit redox potential of Eh=0, taking into consideration the presence and absence of organics respectively. Only the formation of colloidal phases is assumed. The results are presented in

Table 3-11 and Table 3-12.

Table 3-11. Radionuclide speciation and equilibrium concentration for Am and Pu in the SILO. $[ISA]_{aq}=3.8\cdot10^{-5}$ M (considering ISA sorption) and $[EDTA]_T=5.2\cdot10^{-7}$ M. Only species accounting for ≥10% of the dissolved radionuclide speciation are shown.

Porewater	A	B	C	D
pH	13.06	12.60	11.60	9.66
pe	0	0	0	0
$[Ca]_T$ (M)	$1.48\cdot10^{-3}$	$2.00\cdot10^{-2}$	$2.59\cdot10^{-3}$	$4.57\cdot10^{-5}$
Am $[Am]_T=1\cdot10^{-5}$	**$Am(OH)_3$(coll)** $[Am]_{aq}=1.4\cdot10^{-8}$ $Am(OH)_3(ISAH_2)^-$ (63.0%) $Am(OH)_3$ (34.7%)	**$Am(OH)_3$(coll)** $[Am]_{aq}=9.8\cdot10^{-9}$ $Am(OH)_3$ (50.3%) $Am(OH)_3(ISAH_2)^-$ (45.6%)	**$Am(OH)_3$(coll)** $[Am]_{aq}=1.6\cdot10^{-8}$ $Am(OH)_3(ISAH_2)^-$ (56.2%) $Am(OH)_3$ (32.1%) $Am(OH)_2^+$ (11.5%)	**$Am(OH)_3$(coll)** $[Am]_{aq}=1.4\cdot10^{-6}$ $Am(CO_3)_2^-$ (47.5%) $Am(EDTA)^-$ (27.8%) $Am(OH)_2^+$ (11.8%)
Pu $[Pu]_T=1\cdot10^{-5}$	**PuO_2(coll, hyd)** $[Pu]_{aq}=3.5\cdot10^{-8}$ $Pu(OH)_4(ISAH_2)_2^{2-}$ (47.5%) $Pu(OH)_4(ISAH_2)^-$ (39.0%) $Pu(OH)_4$ (13.5%)	**PuO_2(coll, hyd)** $[Pu]_{aq}=1.6\cdot10^{-8}$ $Pu(OH)_4(ISAH_2)^-$ (44.7%) $Pu(OH)_4$ (31.2%) $Pu(OH)_4(ISAH_2)_2^{2-}$ 24.1%)	**PuO_2(coll, hyd)** $[Pu]_{aq}=3.1\cdot10^{-8}$ $Pu(OH)_4(ISAH_2)^-$ (44.4%) $Pu(OH)_4(ISAH_2)_2^{2-}$ (39.6%) $Pu(OH)_4$ (16.0%)	**PuO_2(coll, hyd)** $[Pu]_{aq}=3.5\cdot10^{-8}$ $Pu(OH)_4(ISAH_2)^-$ (43.4%) $Pu(OH)_4(ISAH_2)_2^{2-}$ (39.8%) $Pu(OH)_4$ (14.4%)

Table 3-12. Radionuclide speciation and equilibrium concentration for Am and Pu in the SILO in absence of organics. Only species with ≥10% are shown.

Porewater	A	B	C	D
pH	13.06	12.60	11.60	9.66
pe	0	0	0	0
$[Ca]_T$ (M)	$1.48 \cdot 10^{-3}$	$2.00 \cdot 10^{-2}$	$2.59 \cdot 10^{-3}$	$4.57 \cdot 10^{-5}$
Am $[Am]_T = 1 \cdot 10^{-5}$	**$Am(OH)_3$(coll)** $[Am]_{aq} = 5.2 \cdot 10^{-9}$	**$Am(OH)_3$(coll)** $[Am]_{aq} = 5.4 \cdot 10^{-9}$	**$Am(OH)_3$(coll)** $[Am]_{aq} = 6.8 \cdot 10^{-9}$	**$Am(OH)_3$(coll)** $[Am]_{aq} = 9.8 \cdot 10^{-7}$
	$Am(OH)_3$ (93.9%)	$Am(OH)_3$ (92.5%)	$Am(OH)_3$ (73.4%) $Am(OH)_2^+$ (26.4%)	$Am(CO_3)_2^-$ (66.4%) $Am(OH)_2^+$ (16.4%) $Am(CO_3)^+$ (10.8%)
Pu $[Pu]_T = 1 \cdot 10^{-5}$	**PuO_2(coll, hyd)** $[Pu]_{aq} = 4.8 \cdot 10^{-9}$	**PuO_2(coll, hyd)** $[Pu]_{aq} = 4.9 \cdot 10^{-9}$	**PuO_2(coll, hyd)** $[Pu]_{aq} = 5.0 \cdot 10^{-9}$	**PuO_2(coll, hyd)** $[Pu]_{aq} = 5.1 \cdot 10^{-9}$
	$Pu(OH)_4$ (100%)	$Pu(OH)_4$ (100%)	$Pu(OH)_4$ (100%)	$Pu(OH)_4$ (97.8%)

The following

Table 3-13 and Table 3-14 show the outcome of the calculations considering strong reducing conditions as poised by the anaerobic corrosion of iron. Again the solubility of colloidal hydroxide phases is calculated in the presence and absence of organics in the Silo.

Table 3-13. Radionuclide speciation and equilibrium concentration for Am and Pu in the SILO. $[ISA]_{aq}=3.8\cdot10^{-5}$ M (considering ISA sorption) and $[EDTA]_T=5.2\cdot10^{-7}$ M. Only species accounting for ≥10% of the dissolved radionuclide speciation are shown.

Porewater	A	B	C	D
pH	13.06	12.60	11.60	9.66
pe	-11.79	-11.34	-10.35	-8.45
$[Ca]_T$ (M)	$1.48\cdot10^{-3}$	$2.00\cdot10^{-2}$	$2.59\cdot10^{-3}$	$4.57\cdot10^{-5}$
Am $[Am]_T=1\cdot10^{-5}$	**$Am(OH)_3(coll)$** $[Am]_{aq} = 1.4\cdot10^{-8}$ $Am(OH)_3(ISAH_2)^-$ (63.0%) $Am(OH)_3$ (34.7%)	**$Am(OH)_3(coll)$** $[Am]_{aq} = 9.8\cdot10^{-9}$ $Am(OH)_3$ (50.3%) $Am(OH)_3(ISAH_2)^-$ (45.6%)	**$Am(OH)_3(coll)$** $[Am]_{aq} = 1.6\cdot10^{-8}$ $Am(OH)_3(ISAH_2)^-$ (56.2%) $Am(OH)_3$ (32.1%) $Am(OH)_2^+$ (11.5%)	**$Am(OH)_3(coll)$** $[Am]_{aq} = 1.2\cdot10^{-6}$ $Am(CO_3)_2^-$ (49.2%) $Am(EDTA)^-$ (25.2%) $Am(OH)_2^+$ (12.5%)
Pu $[Pu]_T=1\cdot10^{-5}$	**$Pu(OH)_3(coll)$** $[Pu]_{aq} = 5.7\cdot10^{-8}$ $Pu(OH)_4(ISAH_2)_2^{2-}$ (44.9%) $Pu(OH)_4(ISAH_2)^-$ (36.9%) $Pu(OH)_4$ (12.8%)	**$Pu(OH)_3(coll)$** $[Pu]_{aq} = 2.7\cdot10^{-8}$ $Pu(OH)_4(ISAH_2)^-$ (39.4%) $Pu(OH)_4$ (27.5%) $Pu(OH)_4(ISAH_2)_2^{2-}$ (21.3%) $Pu(OH)_3$ (11.7%)	**$Pu(OH)_3(coll)$** $[Pu]_{aq} = 4.8\cdot10^{-8}$ $Pu(OH)_4(ISAH_2)^-$ (41.5%) $Pu(OH)_4(ISAH_2)_2^{2-}$ (37.0%) $Pu(OH)_4$ (14.9%)	**$Pu(OH)_3(coll)$** $[Pu]_{aq} = 2.6\cdot10^{-7}$ $Pu(CO_3)_3^{3-}$ (32.1%) $Pu(EDTA)^-$ (30.4%) $Pu(CO_3)_2^-$ (16.0%)

Table 3-14. Radionuclide speciation and equilibrium concentration for Am and Pu in the SILO in absence of organics. Only species with ≥10% are shown.

Porewater	A	B	C	D
pH	13.06	12.60	11.60	9.66
pe	-11.79	-11.34	-10.35	-8.45
$[Ca]_T$ (M)	$1.48 \cdot 10^{-3}$	$2.00 \cdot 10^{-2}$	$2.59 \cdot 10^{-3}$	$4.57 \cdot 10^{-5}$
Am $[Am]_T = 1 \cdot 10^{-5}$	**$Am(OH)_3$(coll)** $[Am]_{aq} = 5.2 \cdot 10^{-9}$	**$Am(OH)_3$(coll)** $[Am]_{aq} = 5.4 \cdot 10^{-9}$	**$Am(OH)_3$(coll)** $[Am]_{aq} = 6.8 \cdot 10^{-9}$	**$Am(OH)_3$(coll)** $[Am]_{aq} = 9.0 \cdot 10^{-7}$
	$Am(OH)_3$ (93.9%)	$Am(OH)_3$ (92.5%)	$Am(OH)_3$ (73.4%) $Am(OH)_2^+$ (26.4%)	$Am(CO_3)_2^-$ (66.5%) $Am(OH)_2^+$ (16.9%) $Am(CO_3)^+$ (10.4%)
Pu $[Pu]_T = 1 \cdot 10^{-5}$	**$Pu(OH)_3$(coll)** $[Pu]_{aq} = 1.0 \cdot 10^{-8}$	**$Pu(OH)_3$(coll)** $[Pu]_{aq} = 1.0 \cdot 10^{-8}$	**$Pu(OH)_3$(coll)** $[Pu]_{aq} = 1.0 \cdot 10^{-8}$	**$Pu(OH)_3$(coll)** $[Pu]_{aq} = 1.4 \cdot 10^{-7}$
	$Pu(OH)_4$ (70.5%) $Pu(OH)_3$ (29.5%)	$Pu(OH)_4$ (70.1%) $Pu(OH)_3$ (29.9%)	$Pu(OH)_4$ (69.4%) $Pu(OH)_3$ (30.3%)	$Pu(CO_3)_3^{3-}$ (59.0%) $Pu(CO_3)_2^-$ (29.4%)

The following Figure 3-4 and Figure 3-5 summarise the solubility calculations assuming an excess concentration of 10^{-5} mol·dm^{-3} of total Am and Pu.

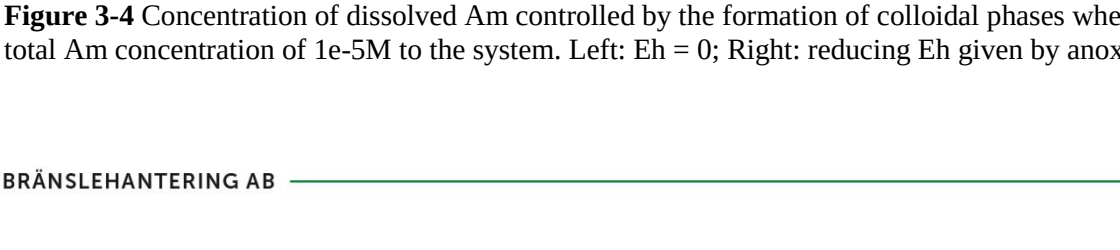

Figure 3-4 Concentration of dissolved Am controlled by the formation of colloidal phases when adding a total Am concentration of 1e-5M to the system. Left: Eh = 0; Right: reducing Eh given by anoxic iron

corrosion and magnetite formation. Black symbols stand for the results in the absence of organics. Open symbols indicate the solubility in the presence of organics.

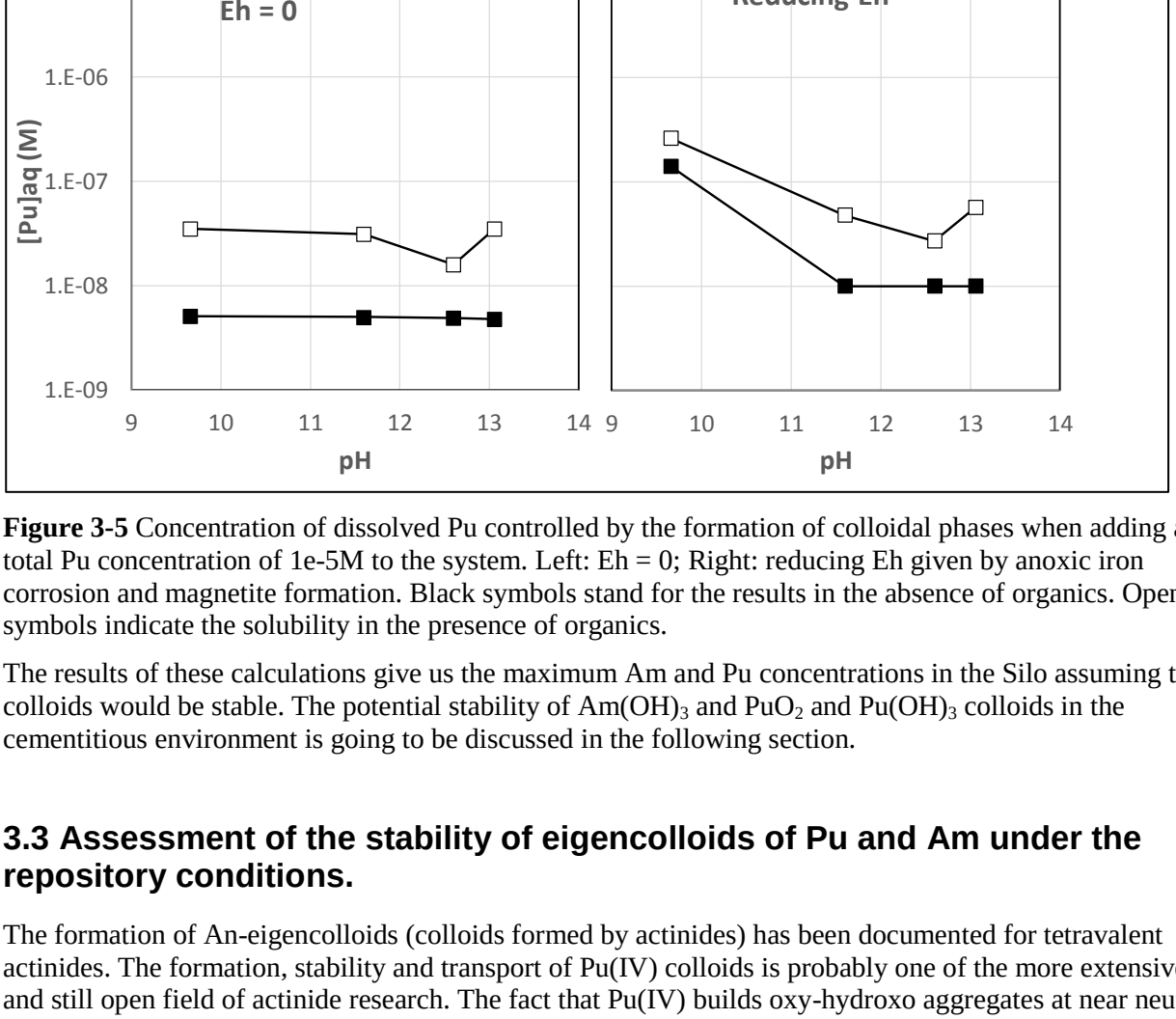

Figure 3-5 Concentration of dissolved Pu controlled by the formation of colloidal phases when adding a total Pu concentration of 1e-5M to the system. Left: Eh = 0; Right: reducing Eh given by anoxic iron corrosion and magnetite formation. Black symbols stand for the results in the absence of organics. Open symbols indicate the solubility in the presence of organics.

The results of these calculations give us the maximum Am and Pu concentrations in the Silo assuming that colloids would be stable. The potential stability of $Am(OH)_3$ and PuO_2 and $Pu(OH)_3$ colloids in the cementitious environment is going to be discussed in the following section.

3.3 Assessment of the stability of eigencolloids of Pu and Am under the repository conditions.

The formation of An-eigencolloids (colloids formed by actinides) has been documented for tetravalent actinides. The formation, stability and transport of Pu(IV) colloids is probably one of the more extensive and still open field of actinide research. The fact that Pu(IV) builds oxy-hydroxo aggregates at near neutral pH values and that they are relatively stable in the neutral to alkaline pH ranges is now well-established (see for instance Zänker and Hennig 2014 and references therein). Observations in the near-neutral to alkaline pH range show aqueous An(IV) concentrations around two log units higher than the ones corresponding to the solubility of amorphous hydroxides, especially when solid-liquid phase separation is not sufficiently effective. Altmaier et al. (2004) studied the formation of colloids in Th(IV) systems and concluded that the solubility of amorphous Th(IV) oxide/hydroxide in near neutral to alkaline chloride solutions was dominated by Th(IV) eigencolloids. In the same reference, the authors summarised that the modelling of the colloidal fraction of tetravalent actinides can be undertaken by assuming a simple equilibrium between the limiting complex and the colloidal species: $An(OH)_4(aq) \Leftrightarrow$"$An(OH)_4(coll)$", with an equilibrium constant that, for Th, they quantified as log K = 2.5±0.8 for An=Th(IV).

The thermodynamic stability of Pu(IV) colloids in the alkaline range has been shown in the solubility studies performed by Neck et al. (2007). The data from Neck et al. (2007) are shown in the following Figure 3-6 (originally taken from the reference)

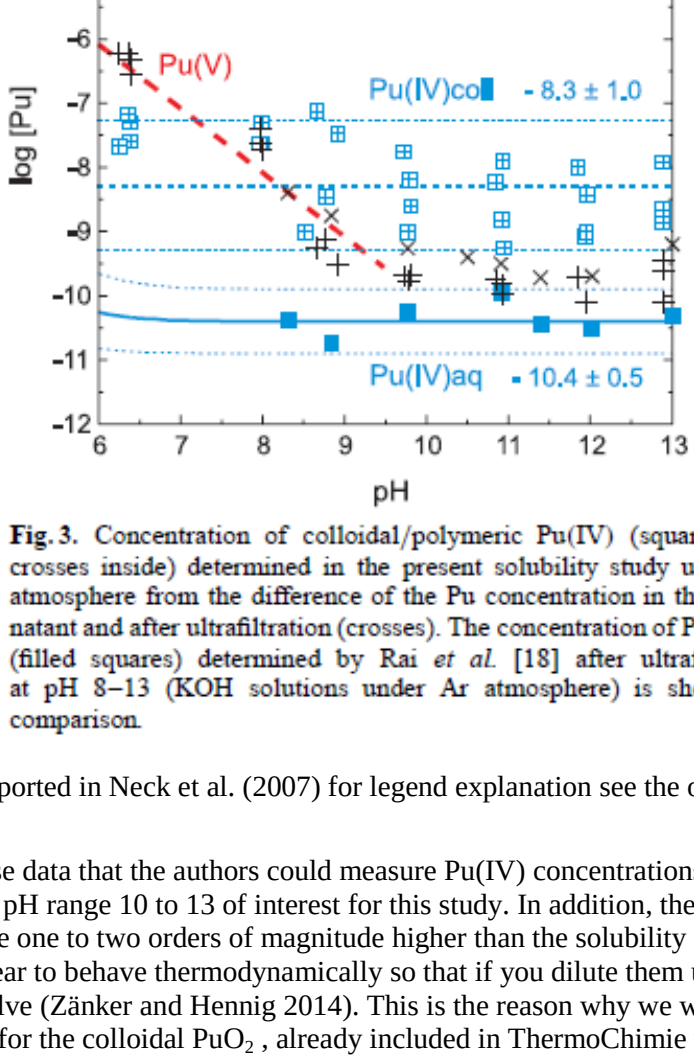

Fig. 3. Concentration of colloidal/polymeric Pu(IV) (squares with crosses inside) determined in the present solubility study under Ar atmosphere from the difference of the Pu concentration in the supernatant and after ultrafiltration (crosses). The concentration of Pu(IV)aq (filled squares) determined by Rai *et al.* [18] after ultrafiltration at pH 8–13 (KOH solutions under Ar atmosphere) is shown for comparison.

Figure 3-6 Data reported in Neck et al. (2007) for legend explanation see the original figure caption inserted.

It is clear from these data that the authors could measure Pu(IV) concentrations stable and rather reproducible in the pH range 10 to 13 of interest for this study. In addition, the measured Pu(IV) concentrations were one to two orders of magnitude higher than the solubility of $Pu(OH)_4(s)$. Furthermore, these particles appear to behave thermodynamically so that if you dilute them under their solubility product, they dissolve (Zänker and Hennig 2014). This is the reason why we were able to propose a solubility constant for the colloidal PuO_2 , already included in ThermoChimie v9b0data base.

It is more difficult to find clear indications of the behaviour of the Pu(IV) colloids in high calcium concentrations. According to Zänker and Hennig (2014), these particles are hydrophilic and their stability is neither influenced by the pH, as indicated by the previous solubility data, nor by the ionic strength. Hence, they are large moieties which behave as aqueous ionic species. In this context it is hard to argue that intrinsic Pu(IV) colloids could be destabilised by the calcium content of cement pore waters.

One very interesting observation made by Knopp et al. (1999) in their LIBD studies of Pu(IV) colloid formation is that there is a clear concentration dependence on the formation of scattering particles. The lower the initial Pu(IV) concentration the lower the breakdown probability, indicating that Pu(IV) colloids are formed only in oversaturated conditions with respect to $Pu(OH)_4(s)$ and not in undersaturated conditions. This would have implications when discussing the effect of Pu sorption onto the cement materials and bentonite, as the resulting concentrations would be much lower than the ones giving rise to oversaturation, so that colloid formation under these conditions is, a priori, not favoured. Scoping

calculations would indicate that the result of sorption of both Pu and Am onto the surface of cement is that concentrations are additionally diminished by half some four orders of magnitude.
This has been done by using the expression:

$$C_f = \frac{C_i V_p}{V_p + M_c K_d}$$

where Vp is pore volume ($7.1\ 10^6$ dm^3), M_c is cement mass ($1.39\ 10^7$ kg), K_d distribution coefficient (10^4 m^3/kg for Am and $3 \cdot 10^4$ for Pu), according to Ochs et al. (2014). The final concentrations obtained in sorption equilibrium with cement are; $5 \cdot 10^{-12}$ mol dm^{-3} for Am and $9.7\ 10^{-14}$ mol dm^{-3} for Pu, assuming the maximum initial concentrations obtained in the previous solubility calculations. This is C_i(Am) = 10^{-7} mol·dm^{-3} and C_i(Pu) = $1.654 \cdot 10^{-9}$ mol·$dm^{-3.}$

This means that taking into consideration sorption onto the cement in the Silo decreases the radionuclide concentration in some 4 orders of magnitude. Hence, the formation of eigencolloids would be not favoured under these circumstances.

In addition, the case of actinide(III) colloids is quite different. The thermodynamic stability of Am(III) and Pu(III) colloids is relatively lower as compared to Pu(IV) colloids. This is probably due to the fact that the stability of $An(OH)_3(s)$ is much lower than the stability of $An(OH)_4(s)$. Early evidences of this relative lower stability are the readiness of colloidal americium to dissolve under acidic conditions compared to a much slower process for colloidal plutonium (Tsvetaeva et al. 1986)

Am(III) colloids have been extensively studied in the past (Olofsson et al. 1983, Vilks and Drew 1986). The data indicates that they become unstable with increasing ionic strength and alkalinity but there also indications that this trend is reversed over pH 12. The centrifugation data obtained by Olofsson et al. (1983) is shown in the Figure 3-7, Figure 3-8 and Figure 3-9.

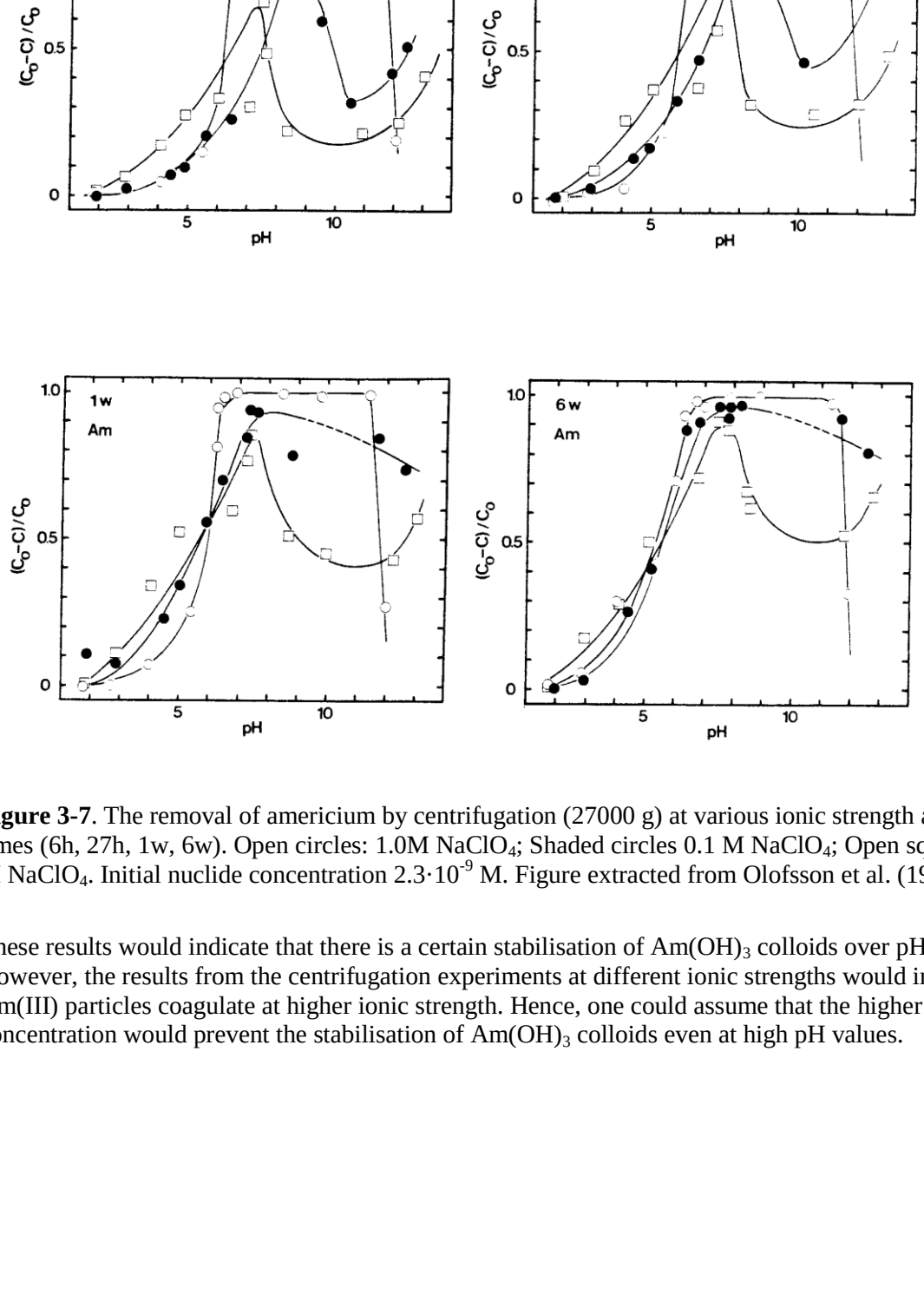

Figure 3-7. The removal of americium by centrifugation (27000 g) at various ionic strength at storage times (6h, 27h, 1w, 6w). Open circles: 1.0M $NaClO_4$; Shaded circles 0.1 M $NaClO_4$; Open squares: 0.01 M $NaClO_4$. Initial nuclide concentration $2.3 \cdot 10^{-9}$ M. Figure extracted from Olofsson et al. (1983).

These results would indicate that there is a certain stabilisation of $Am(OH)_3$ colloids over pH 11. However, the results from the centrifugation experiments at different ionic strengths would imply that the Am(III) particles coagulate at higher ionic strength. Hence, one could assume that the higher sodium concentration would prevent the stabilisation of $Am(OH)_3$ colloids even at high pH values.

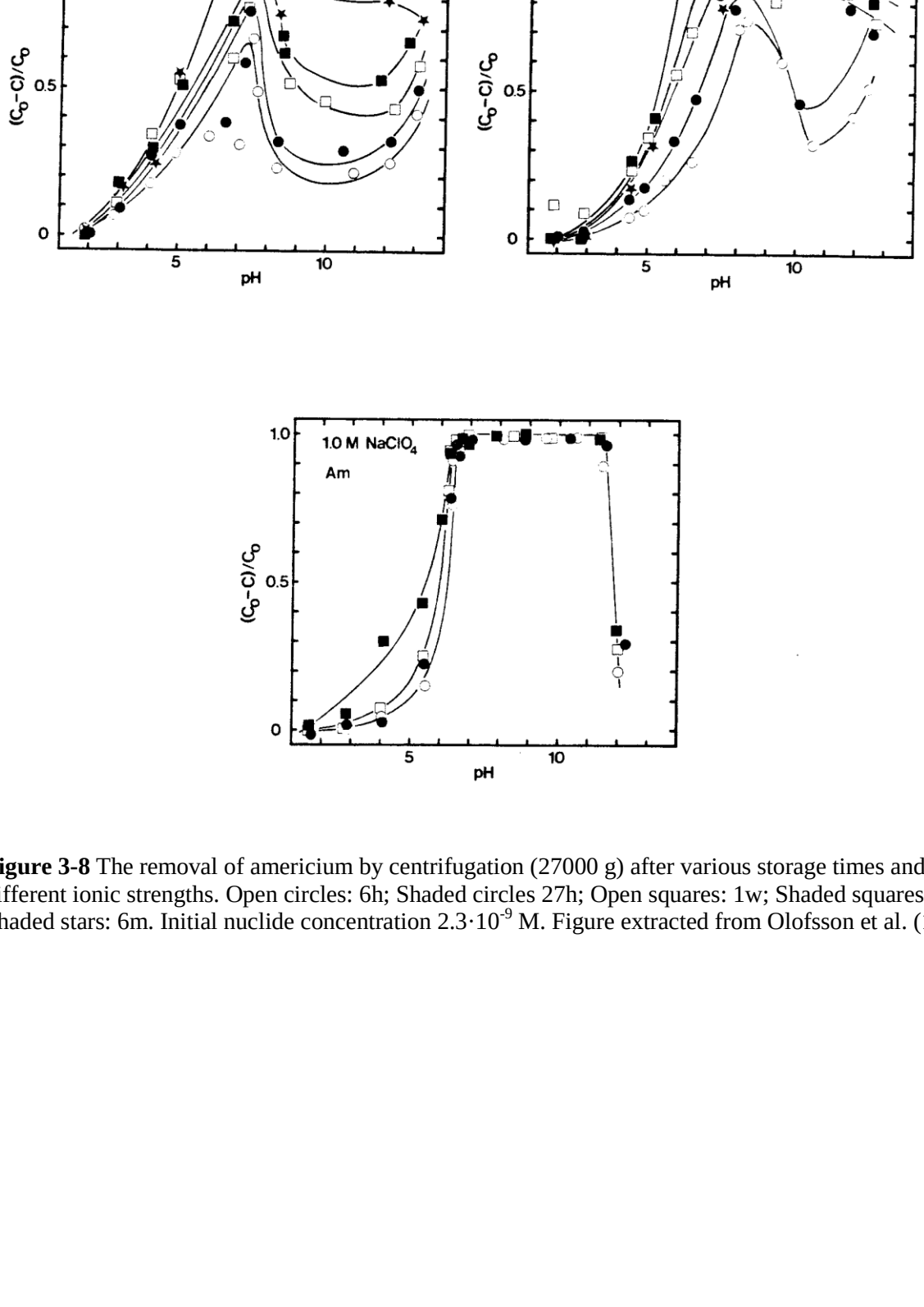

Figure 3-8 The removal of americium by centrifugation (27000 g) after various storage times and at different ionic strengths. Open circles: 6h; Shaded circles 27h; Open squares: 1w; Shaded squares: 6w; Shaded stars: 6m. Initial nuclide concentration $2.3 \cdot 10^{-9}$ M. Figure extracted from Olofsson et al. (1983).

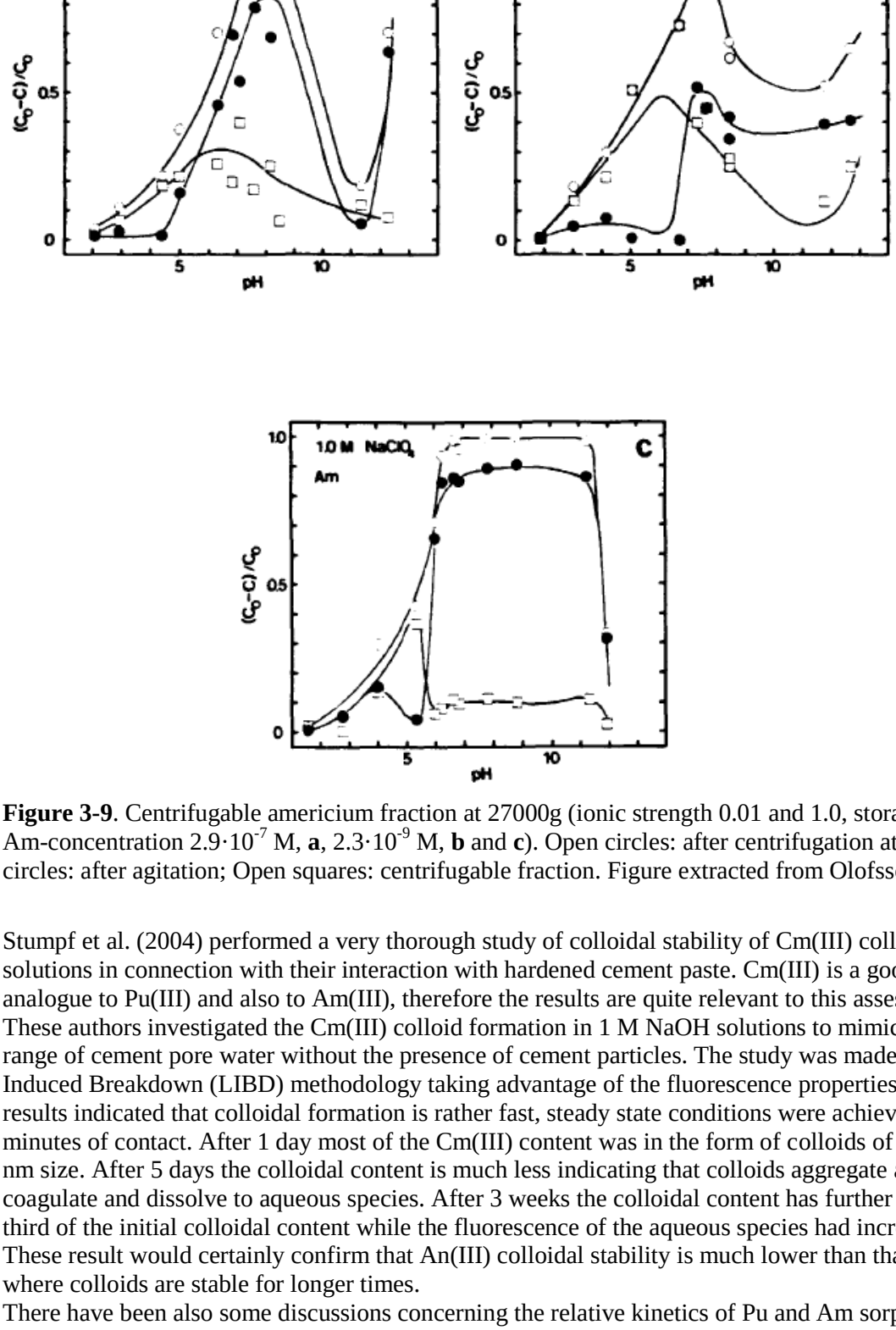

Figure 3-9. Centrifugable americium fraction at 27000g (ionic strength 0.01 and 1.0, storage time 6w, Am-concentration $2.9 \cdot 10^{-7}$ M, **a**, $2.3 \cdot 10^{-9}$ M, **b** and **c**). Open circles: after centrifugation at 27000g; Shaded circles: after agitation; Open squares: centrifugable fraction. Figure extracted from Olofsson et al. (1983).

Stumpf et al. (2004) performed a very thorough study of colloidal stability of Cm(III) colloids in alkaline solutions in connection with their interaction with hardened cement paste. Cm(III) is a good chemical analogue to Pu(III) and also to Am(III), therefore the results are quite relevant to this assessment.
These authors investigated the Cm(III) colloid formation in 1 M NaOH solutions to mimic the initial pH range of cement pore water without the presence of cement particles. The study was made using the Laser Induced Breakdown (LIBD) methodology taking advantage of the fluorescence properties of Cm(III). The results indicated that colloidal formation is rather fast, steady state conditions were achieved after 50 minutes of contact. After 1 day most of the Cm(III) content was in the form of colloids of some 70-100 nm size. After 5 days the colloidal content is much less indicating that colloids aggregate and eventually coagulate and dissolve to aqueous species. After 3 weeks the colloidal content has further decreased to a third of the initial colloidal content while the fluorescence of the aqueous species had increased.
These result would certainly confirm that An(III) colloidal stability is much lower than that of An(IV) where colloids are stable for longer times.
There have been also some discussions concerning the relative kinetics of Pu and Am sorption on cement compared to the aqueous complex reactions and to which extent the faster sorption reaction would hamper the hydrolysis reactions in solution and the subsequent colloid formation. However, according to the review performed by Bruno (1997) the characteristic reaction times of both processes are in the range of

seconds to minutes. As a matter of fact, in many cases surface complexes mimic the aquatic speciation and the metals are sorbed in their complexed fashion. Hence, this argument cannot be used to disregard the potential formation of Pu and Am colloids in the presence of cement.

3.4 Assessment and quantification of the potential partition of eigencolloids in the cement surface.

While the potential sorption of the dissolved content of radionuclides and the impact of organic ligands on it has been largely studied (see for instance Ochs et al. 2014), there is much less information regarding the interaction of radionuclide colloids with cement.

Jakubick et al. (1986) studied the sorption of Am(III) and Pu(IV) on cement. They have shown that the surface distribution pattern of Pu follows the concrete structure selectively. The sorption was preferential in the cement paste rather than on aggregates, both for normal and high-density concrete.

Konishi et al. (1997) reported on investigations of the sorption behaviour of Pu(IV) and Np(V) on cement and they described quite high Kd values for both radionuclides, starting with 10^5 ml/g on fresh cement and decreasing to 10^4 ml/g for Pu(IV) as alteration proceeded. They indicated the presence of Np(V) colloids in contact with cement and pointed out that those colloids were filtered. No information on Pu(IV) colloids is available on the English translation of the abstract, as the original work is in Japanese.

Baston et al. (1994) performed a number of Am and Pu sorption experiments on cement. Comparatively Pu sorption was stronger than Am sorption in the concrete phases. The experiments were carried out at very low radionuclide concentrations precluding the formation of colloidal phases. The authors explained the sorption behaviour of both nuclides by assuming surface complexation to the silanol groups. However, the authors assumed that Pu(IV) aqueous speciation was dominated by a $Pu(OH)_2O_2^{2-}$ complex which is not in line with our current knowledge on Pu(IV) chemistry. Nevertheless, the results would indicate that the surface complex of $Pu(OH)_4$ with the silanol groups is quite strong.

Aggarwal et al. (2000) found that Pu and Am sorption increased with increasing fraction of Ordinary Portland Cement (OPC) and decreased with alteration.

Wieland et al. (2004) performed a thorough investigation of the interaction of cement with Cs, Sr and Th, but the emphasis was on the role of cement colloids on the mobilisation of the dissolved elements.

As mentioned in the previous section, Stumpf et al. (2004) performed a thorough investigation of the interaction of Cm(III) with hardened cement paste (HCP) by using LIBD and fluorescence spectroscopy as a follow up of the work the authors had previously done with $Ca(OH)_2$(s) (Tits et al. 2003). The outcome of this study indicated that Cm(III) colloids become unstable in the presence of HCP. Initially, Cm(III) was sorbed on the HCP surface as a Cm(III) hydroxide surface species but gradually became incorporated into the HCP structure as surface precipitates.

Wang et al. (2009) carried out an extensive review of the Kd/Rd values for Pu sorption on cement. In general, most of the selected data is at Pu levels below saturation with respect to $Pu(OH)_4$(s) and consequently no colloids could be expected as most of the Pu(IV) is in the form of $Pu(OH)_4$(aq). However, the strong sorption intensity of $Pu(OH)_4$(aq) is an indication that the analogous colloidal phase could behave in a similar way.

In recent years the interaction of Pu(IV) with different mineral surfaces has been studied in depth. There is an agreement that intrinsic Pu(IV) colloids form 2-5 nm nanocolloids (Kersting 2013) and as we have already shown they are stable in the neutral to alkaline pH range. The TEM work by Powell et al. (2011) showed that these colloids are crystalline and become easily aggregated in mats of 2-5 nm (see Figure 3-10).

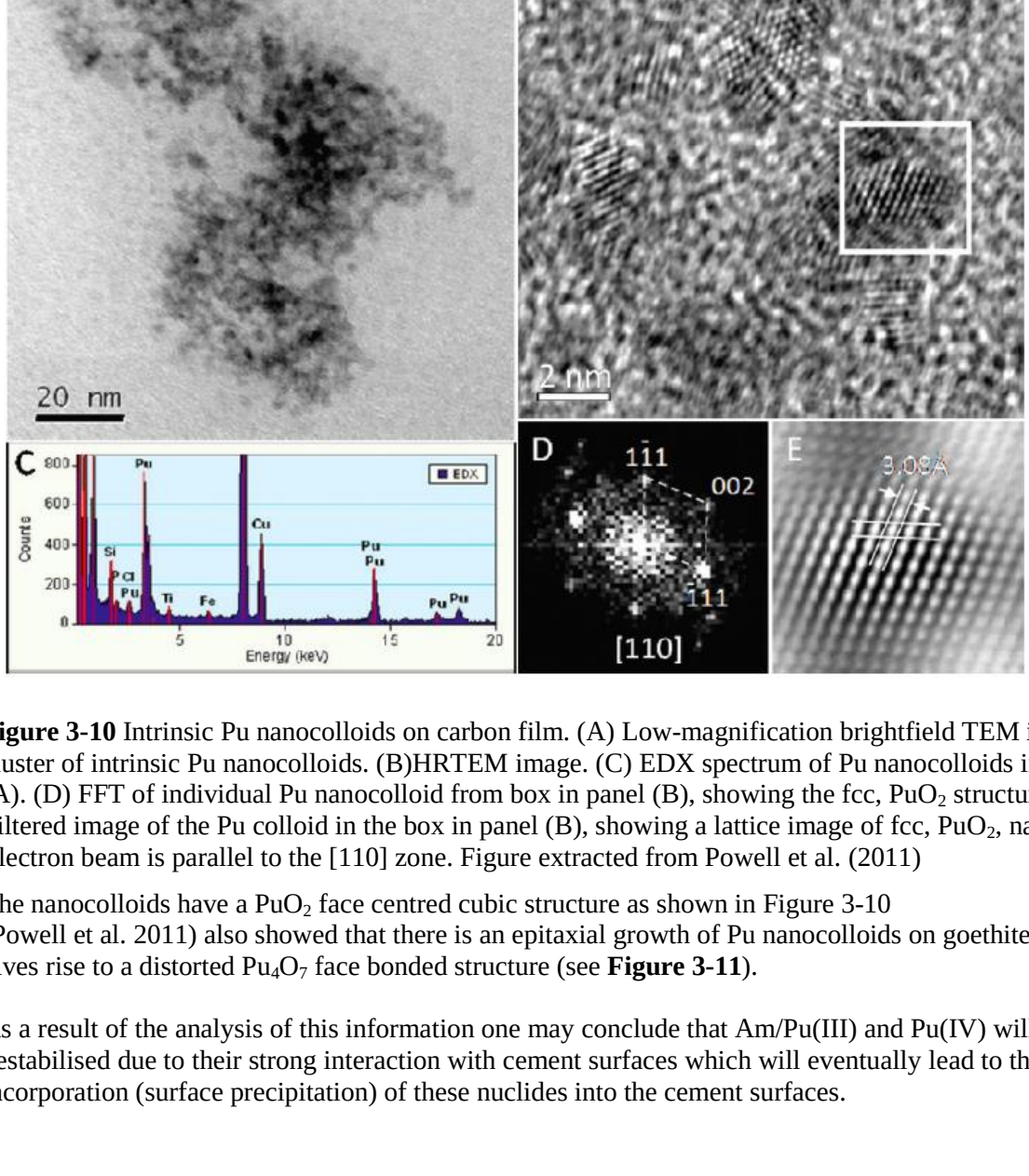

Figure 3-10 Intrinsic Pu nanocolloids on carbon film. (A) Low-magnification brightfield TEM image of a cluster of intrinsic Pu nanocolloids. (B)HRTEM image. (C) EDX spectrum of Pu nanocolloids in panel (A). (D) FFT of individual Pu nanocolloid from box in panel (B), showing the fcc, PuO_2 structure. (E) Filtered image of the Pu colloid in the box in panel (B), showing a lattice image of fcc, PuO_2, nanocolloid. Electron beam is parallel to the [110] zone. Figure extracted from Powell et al. (2011)

The nanocolloids have a PuO_2 face centred cubic structure as shown in Figure 3-10 (Powell et al. 2011) also showed that there is an epitaxial growth of Pu nanocolloids on goethite which gives rise to a distorted Pu_4O_7 face bonded structure (see **Figure 3-11**).

As a result of the analysis of this information one may conclude that Am/Pu(III) and Pu(IV) will be destabilised due to their strong interaction with cement surfaces which will eventually lead to the incorporation (surface precipitation) of these nuclides into the cement surfaces.

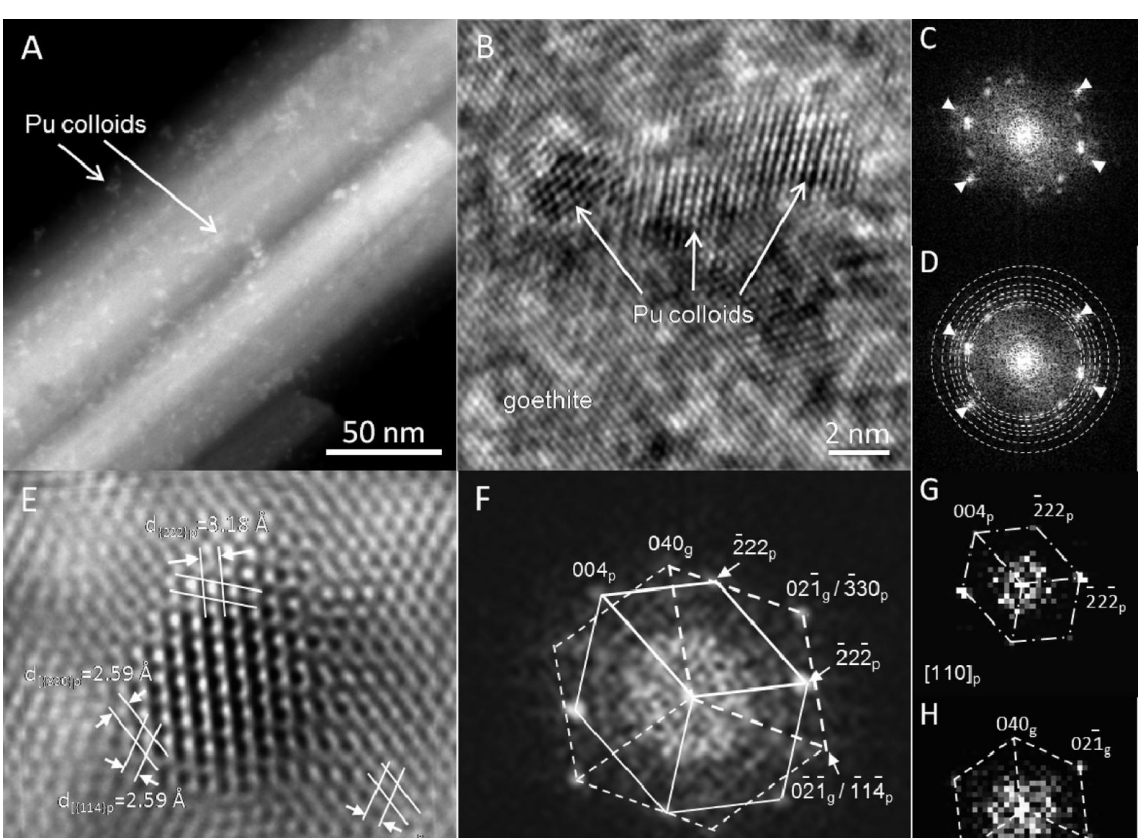

Figure 3-11 Pu nanocolloids formed in situ on goethite. (A) HAADF STEM image showing Pu nanocolloids (with highly bright contrast) growing on goethite. (B)HRTEMimage of Pu4O7 nanocolloids on goethite. (C,D) FFT of the HRTE Mimage shown in panel (B), in which the reflections indicated by arrowheads are from goethite, and reflections located on rings are the bcc, Pu4O7 structure. (E) HRTEM image of an individual Pu4O7 nanoparticle on goethite, showing the lattice orientation relationship between Pu4O7 and goethite. Lighter background is the host goethite, and the darker image is the single Pu colloid. Lower case g and p next to the d-spacing denotes the phase goethite and Pu nanocolloid, respectively. There is a periodic relationship at 2.59 Å between the host goethite {021} and the Pu {114} or Pu {330} crystal plane. (F) FFT of the HRTEM image shown in panel (E), showing the orientation relationship between the two phases. (G,H) FFT of the Pu4O7 colloid and FFT of goethite, respectively, from panel (E).are from goethite, and reflections located on rings are the fcc, PuO2. Figure extracted from Powell et al. (2011).

This would indicate the formation of a stronger surface binding and therefore the attachment of the Pu(IV) colloids onto the goethite structure, such behaviour could also be expected on the surface of cement phases.

3.5Assessment of the stability and transport of the eigencolloids in the bentonite barrier of the Silo.

Filtering effects on the Silo bentonite can be divided in physical and chemical filtering. Physical filtering of bentonite is a function of bentonite compaction. In the case of the low compacted bentonite in the Silo, physical filtering of 2-4 nm particles can be excluded.

Chemical filtering would be the effect of the montmorillonite surface on the stability of Am(III) and Pu(III)/(IV) colloids as a result of their chemical sorption (surface complexation) on the montmorillonite surface.

The final report of the Project Kollorado-2 (Huber et al. 2014) provides many data of interaction of colloids of radionuclides with bentonite.

The alkaline cement pore water that could contain the radionuclide colloids will interact with the bentonite porewater creating a strong chemical gradient. This gradient by itself could constitute a destabilisation factor for the potential radionuclide eigen colloids. In addition, the strong sorption of the actinide hydroxo complexes onto the montmorillonite surface will contribute to a more extensive destabilisation of the colloids. For instance, Begg et al. (2013) have shown that Pu(IV) sorbs quantitatively onto the montmorillonite in a matter of minutes.
The most comprehensive and extensive work on the sorption of radionuclides on bentonite has been performed by Bradbury and Baeyens (2005a, b). The authors have developed a consistent and thermodynamic surface complexation model for a number of radionuclides including Am(III). In addition, they were able to extend their model to other chemical elements that had not been properly measured, including Pu(III) and Pu(IV). In either case, the results of the model indicated a strong (Am(III)/Pu(III)) to very strong (Pu(IV)) sorption onto montmorillonite in the neutral to alkaline pH range.
Hence, similarly to the reasoning we have made concerning the interaction of Am and Pu colloids with cement, the surface interaction with bentonite will destabilise their colloids through sorption acting as a chemical filter.

3.6Assessment of the stability of cementitious colloids under repository conditions

To our knowledge the most comprehensive and quantitative investigation of the generation and impact of cement colloids on radionuclide migration was published in 2004 by Wieland et al.
The main conclusions of this study were:

1. Cement colloids have a composition similar to the one of the CSH phases
2. Colloid concentrations are typically below 0.1 mg l^{-1} in cement porewaters
3. For most of the radionuclides studied, including Th(IV) the contribution of cement colloids to radionuclide mobilisation is relatively small due to the strong Th(IV) sorption and the limited colloidal concentration.

Hence, as a follow up of what it was already stated in SKB (2014b), the stability of cementitious colloids is low, they tend to coagulate in days, and their impact on potential mobilisation of Am(III) and Pu(IV) will be limited.

4 Conclusions

Considering the inventory of Pu in the various parts of the repository and particularly in the Silo, the calculated porewater concentrations are under the saturation limit for the formation of colloidal phases, hence the formation of intrinsic Pu(IV) colloids is unlikely.
In the case of Am(III), the porewater concentrations calculated from the actual inventory at the Silo are oversaturated with respect to the colloidal phase and therefore the formation of Am(III) colloids is possible.
While the stability of Pu(IV) intrinsic colloids is rather high in the alkaline conditions expected in the cement porewaters, this is not the case for Am(III) and Pu(III) colloids which become destabilised much faster in the relatively high ionic strength and alkalinity conditions.
In the presence of cement and bentonite surfaces the actinide colloids become destabilised due to sorption and surface precipitation processes which incorporate the radionuclides into the cement phases structure.
The concentration of cementitious colloids is relatively low and its composition mimics the corresponding CSH phases. The contribution of these cementitious colloids to Am(III) and Pu(IV) transport is deemed to be rather small.

References

Aggarwal S, Angus M J, Ketchen J, 2000. Sorption of radionuclides onto specific mineral phases present in repository cement. NIREX Safety Studies Report NSS/R312, UK Nirex.

Altmaier M, Neck V, Fanghänel T, 2004. Solubility and colloid formation of Th(IV) in concentrated NaCl and $MgCl_2$ solution. Radiochimica Acta 92, 537–543.

Baston G M N, Berry J A, Brownsword M, Heath T G, Tweed C J, Williams S J, 1994. Sorption of plutonium and americium on repository, backfill and geological materials relevant to the JNFL low-level radioactive waste repository at Rokkasho-Mura. In Murakami T, Ewing R C (eds). Scientific basis for nuclear waste management XVIII: symposium held in Kyoto, Japan, 23–27 October 1994. Pittsburgh, PA: Materials Research Society. (Materials Research Society Symposium Proceedings 353), 957.

Begg J D, Zavarin M, Zhao P, Tumey S J, Powell B, Kersting A B, 2013. Pu(V) and Pu(IV) sorption to montmorillonite. Environmental Science & Technology 47, 5146–5153.

Bradbury M H, Baeyens B, 2005a. Modelling the sorption of Mn(II), Co(II), Ni(II), Zn(II), Cd(II), Eu(III), Am(III), Sn(IV), Th(IV), Np(V) and U(VI) on montmorillonite: linear free energy relationships and estimates of surface binding constants for some selected heavy metals and actinides. Geochimica et Cosmochimica Acta 69, 875–892.

Bradbury M H, Baeyens B, 2005b. Experimental measurements and modeling of sorption competition on montmorillonite. Geochimica et Cosmochimica Acta 69, 4187–4197.

Cronstrand P, 2014. Evolution of pH in SFR 1. SKB R-14-01, Svensk Kärnbränslehantering AB.

Duro L, Grivé M, Domènech C, Roman-Ross G, Bruno J, 2012. Assessment of the evolution of the redox conditions in SFR 1. SKB TR-12-12, Svensk Kärnbränslehantering AB.

Giffaut E, Grivé M, Blanc P, Vieillard P, Colàs E, Gailhanou H, Gaboreau S, Marty N, Madé B, Duro L, 2014. Andra thermodynamic data for performance assessment: ThermoChimie. Applied Geochemistry 49, 225–236.

Jakubick A T, Gillham R W, Kahl I, Robin M, 1986. Attenuation of Pu, Am, Cs and Sr mobility in concrete. In Bates J K, Seefeldt W B (eds). Scientific basis for nuclear waste management X: symposium held in Boston, Massachusetts, USA, 1–4 December 1986. Pittsburgh, PA: Materials Research Society. (Materials Research Society Symposium Proceedings 84), 355.

Keith-Roach M, Lindgren M, Källström K, 2014. Assessment of complexing agent concentrations in SFR. SKB R-14-03, Svensk Kärnbränslehantering AB.

Kersting A B, 2013. Plutonium transport in the environment. Inorganic Chemistry 52, 3533–3546.

Knopp R, Neck V, Kim J I, 1999. Solubility, hydrolysis and colloid formation of plutonium(IV). Radiochimica Acta 86, 101–108.

Konishi M, Sakamoto Y, Senoo M, Moriyama N, 1997. Interaction between cementitious materials and Np(V) or Pu(IV). Journal of Nuclear Fuel Cycle and Environment 4, 47–55.

Huber F, Noseck U, Schäfer T (eds), 2014. Colloid/nanoparticle formation and mobility in the context of deep geological nuclear waste disposal. Project KOLLORADO-2 Final Report. KIT Scientific Report 7645, Karlsruhe Institute of Technology.

Neck V, Altmaier M, Seibert A, Yun J I, Marquardt C M, Fanghänel T, 2007. Solubility and redox reactions of Pu(IV) hydrous oxide: evidence for the formation of PuO_{2+x} (s, hyd). Radiochimica Acta 95, 193–207.

Ochs M, Colàs E, Grivé M, Olmeda J, Campos I, Bruno J, 2014. Reduction of radionuclide uptake in hydrated cement systems by organic complexing agents: Selection of reduction factors and speciation calculations. SKB R-14-22, Svensk Kärnbränslehantering AB.

Olofsson U, Allard B, Bengtsson, M, Torstenfelt B, Andersson K, 1983. Formation and properties of actinide colloids. SKBF/KBS TR 83-08, Svensk Kärnbränslehantering AB.

Parkhurst D L, Appelo C A J, 2013. Description of input and examples for PHREEQC version 3: a computer program for speciation, batch-reaction, one-dimensional transport, and inverse geochemical calculations. Denver, CO: U.S. Geological Survey. (Techniques and Methods 6-A43)

Powell B A, Dai Z, Zavarin M, Zhao P, Kersting A B, 2011. Stabilization of plutonium nano-colloids by epitaxial distortion on mineral surfaces. Environmental Science & Technology 45, 2698–2703.

SKB, 2008. Safety analysis SFR 1. Long-term safety. SKB R-08-130, Svensk Kärnbränslehantering AB

SKB, 2014a. Initial state report for the safety assessment SR-PSU. SKB TR-14-02, Svensk Kärnbränslehantering AB.

SKB, 2014b. Waste form and packaging process report for the safety assessment SR-PSU. SKB TR-14-03, Svensk Kärnbränslehantering AB.

Stumpf T, Tits J, Walther C, Wieland E, Fanghänel T, 2004. Uptake of trivalent actinides (curium(III)) by hardened cement paste: a time-resolved laser fluorescence spectroscopy study. Journal of Colloid and Interface Science 276, 118–124.

Tsvetaeva N E, Filin V M, Ragimov T K, Rudaya L Y, Shapiro K Y, Shcherbakov B Y, 1986. Comparative behavior of americium and plutonium in wastewater (Engl. transl.). Soviet Radiochemistry 28, 114–118.

Tits J, Stumpf T, Rabung T, Wieland E, Fanghänel T, 2003. Uptake of Cm(III) and Eu(III) by calcium silicate hydrates: a solution chemistry and time-resolved laser fluorescence spectroscopy study. Environmental Science & Technology 37, 3568–3573.

Vilks P, Drew D J, 1986. The effect of colloids on actinide migration. In Proceedings of the 2nd International Conference on Radioactive Waste Management, Winnipeg, Canada, 7–11 September 1986. Canadian Nuclear Society, 667–673.

Wang L, Martens E, Jacques D, De Cannière P, Berry J, Mallants D, 2009. Review of sorption values for the cementitious near field of a near surface radioactive waste disposal facility. NIROND-TR 2008-23 E, ONDRAF/NIRAS, Belgium

Wieland E, Tits J, Bradbury M H, 2004. The potential effect of cementitious colloids on radionuclide mobilisation in a repository for radioactive waste. Applied Geochemistry 19, 119–135.

Zänker H, Hennig C, 2014. Colloid-borne forms of tetravalent actinides: a brief review. Journal of Contaminant Hydrology 157, 87–105.

Appendix A: Speciation and solubility calculations with porewaters, organic ligands and radionuclide inventories for each part of the repository.

Table A 1. Radionuclide speciation and equilibrium concentration for Am and Pu in the SILO. $[ISA]_{aq}=3.8\cdot10^{-5}$ M (considering ISA sorption). Only species accounting for ≥10% of the dissolved radionuclide speciation are shown.

Porewater	A	B	C	D
pH	13.06	12.60	11.60	9.66
pe	0	0	0	0
$[Ca]_T$ (M)	$1.49\cdot10^{-3}$	$2.00\cdot10^{-2}$	$2.59\cdot10^{-3}$	$4.57\cdot10^{-5}$
Am $[Am]_T=1.1\cdot10^{-7}$	**$Am(OH)_3$(coll)** $[Am]_{aq}=1.4\cdot10^{-8}$	**$Am(OH)_3$(coll)** $[Am]_{aq}=9.8\cdot10^{-9}$	**$Am(OH)_3$(coll)** $[Am]_{aq}=1.6\cdot10^{-8}$	**No precipitation** $[Am]_{aq}=1.1\cdot10^{-7}$
	$Am(OH)_3(ISAH_2)^-$ (63.1%) $Am(OH)_3$ (34.7%)	$Am(OH)_3$ (50.3%) $Am(OH)_3(ISAH_2)^-$ (45.6%)	$Am(OH)_3(ISAH_2)^-$ (56.3%) $Am(OH)_3$ (32.1%) $Am(OH)_2^+$ (11.5%)	$Am(CO_3)_2^-$ (65.8%) $Am(OH)_2^+$ (16.6%) $Am(CO_3)^+$ (10.2%)
	$Am(OH)_3$(am) $[Am]_{aq}=1.4\cdot10^{-9}$	**$Am(OH)_3$(am)** $[Am]_{aq}=9.8\cdot10^{-10}$	**$Am(OH)_3$(am)** $[Am]_{aq}=1.6\cdot10^{-9}$	**$Am(OH)_3$(am)** $[Am]_{aq}=9.1\cdot10^{-8}$
	$Am(OH)_3(ISAH_2)^-$ (63.0%) $Am(OH)_3$ (34.7%)	$Am(OH)_3$ (50.3%) $Am(OH)_3(ISAH_2)^-$ (45.6%)	$Am(OH)_3(ISAH_2)^-$ (56.3%) $Am(OH)_3$ (32.1%) $Am(OH)_2^+$ (11.5%)	$Am(CO_3)_2^-$ (65.8%) $Am(OH)_2^+$ (16.6%) $Am(CO_3)^+$ (10.2%)
Pu $[Pu]_T=6.5\cdot10^{-9}$ ***PuO_2(coll, hyd) is never oversaturated***	**$Pu(OH)_4$(am)** $[Pu]_{aq}=3.4\cdot10^{-9}$	**$Pu(OH)_4$(am)** $[Pu]_{aq}=1.6\cdot10^{-9}$	**$Pu(OH)_4$(am)** $[Pu]_{aq}=3.1\cdot10^{-9}$	**$Pu(OH)_4$(am)** $[Pu]_{aq}=3.5\cdot10^{-9}$
	$Pu(OH)_4(ISAH_2)_2^{2-}$ (47.5%) $Pu(OH)_4(ISAH_2)^-$ (39.0%) $Pu(OH)_4$ (13.5%)	$Pu(OH)_4(ISAH_2)^-$ (44.7%) $Pu(OH)_4$ (31.1%) $Pu(OH)_4(ISAH_2)_2^{2-}$ (24.2%)	$Pu(OH)_4(ISAH_2)^-$ (44.4%) $Pu(OH)_4(ISAH_2)_2^{2-}$ (39.6%) $Pu(OH)_4$ (16.0%)	$Pu(OH)_4(ISAH_2)^-$ (43.5%) $Pu(OH)_4(ISAH_2)_2^{2-}$ (39.9%) $Pu(OH)_4$ (14.4%)

Table A 2. Radionuclide speciation and equilibrium concentration for Am and Pu in the SILO. $[EDTA]_{aq}=5.2\cdot10^{-7}$ M. Only species with ≥10% are shown.

Porewater	A	B	C	D
pH	13.06	12.60	11.60	9.66
pe	0	0	0	0
$[Ca]_T$ (M)	$1.49\cdot10^{-3}$	$2.00\cdot10^{-2}$	$2.59\cdot10^{-3}$	$4.57\cdot10^{-5}$
Am $[Am]_T=1.1\cdot10^{-7}$	**$Am(OH)_3$(coll)** $[Am]_{aq}=5.2\cdot10^{-9}$	**$Am(OH)_3$(coll)** $[Am]_{aq}=5.4\cdot10^{-9}$	**$Am(OH)_3$(coll)** $[Am]_{aq}=6.8\cdot10^{-9}$	**No precipitation** $[Am]_{aq}=1.1\cdot10^{-7}$
	$Am(OH)_3$ (93.9%)	$Am(OH)_3$ (92.5%)	$Am(OH)_3$ (73.4%) $Am(OH)_2^+$ (26.4%)	$Am(EDTA)^-$ (54.1%) $Am(CO_3)_2^-$ (30.6%)
	$Am(OH)_3$(am) $[Am]_{aq}=5.2\cdot10^{-10}$	**$Am(OH)_3$(am)** $[Am]_{aq}=5.4\cdot10^{-10}$	**$Am(OH)_3$(am)** $[Am]_{aq}=6.8\cdot10^{-10}$	**No precipitation** $[Am]_{aq}=1.1\cdot10^{-7}$
	$Am(OH)_3$ (93.9%)	$Am(OH)_3$ (92.5%)	$Am(OH)_3$ (73.4%) $Am(OH)_2^+$ (26.4%)	$Am(EDTA)^-$ (54.1%) $Am(CO_3)_2^-$ (30.6%)
Pu $[Pu]_T=6.5\cdot10^{-9}$	**PuO_2(coll, hyd)** $[Pu]_{aq}=4.8\cdot10^{-9}$	**PuO_2(coll, hyd)** $[Pu]_{aq}=4.9\cdot10^{-9}$	**PuO_2(coll, hyd)** $[Pu]_{aq}=5.0\cdot10^{-9}$	**PuO_2(coll, hyd)** $[Pu]_{aq}=5.1\cdot10^{-9}$
	$Pu(OH)_4$ (100%)	$Pu(OH)_4$ (100%)	$Pu(OH)_4$ (100%)	$Pu(OH)_4$ (97.9%)
	$Pu(OH)_4$(am) $[Pu]_{aq}=4.8\cdot10^{-10}$	**$Pu(OH)_4$(am)** $[Pu]_{aq}=4.9\cdot10^{-10}$	**$Pu(OH)_4$(am)** $[Pu]_{aq}=5.0\cdot10^{-10}$	**$Pu(OH)_4$(am)** $[Pu]_{aq}=5.1\cdot10^{-10}$
	$Pu(OH)_4$ (100%)	$Pu(OH)_4$ (100%)	$Pu(OH)_4$ (100%)	$Pu(OH)_4$ (97.9%)

Table A 3. Radionuclide speciation and equilibrium concentration for Am and Pu in the SILO. $[ISA]_{aq}=3.8\cdot10^{-5}$ M (considering ISA sorption) and $[EDTA]_T=5.2\cdot10^{-7}$ M. Only species accounting for ≥10% of the dissolved radionuclide speciation are shown.

Porewater	A	B	C	D
pH	13.06	12.60	11.60	9.66
pe	0	0	0	0
$[Ca]_T$ (M)	$1.49\cdot10^{-3}$	$2.00\cdot10^{-2}$	$2.59\cdot10^{-3}$	$4.57\cdot10^{-5}$
Am $[Am]_T=1.1\cdot10^{-7}$	**$Am(OH)_3$(coll)** $[Am]_{aq}=1.4\cdot10^{-8}$	**$Am(OH)_3$(coll)** $[Am]_{aq}=9.8\cdot10^{-9}$	**$Am(OH)_3$(coll)** $[Am]_{aq}=1.6\cdot10^{-8}$	**No precipitation** $[Am]_{aq}=1.1\cdot10^{-7}$
	$Am(OH)_3(ISAH_2)^-$ (63.1%) $Am(OH)_3$ (34.7%)	$Am(OH)_3$ (50.3%) $Am(OH)_3(ISAH_2)^-$ (45.6%)	$Am(OH)_3(ISAH_2)^-$ (56.3%) $Am(OH)_3$ (32.1%) $Am(OH)_2^+$ (11.5%)	$Am(EDTA)^-$ (53.8%) $Am(CO_3)^+$ (30.4%)
	$Am(OH)_3$(am) $[Am]_{aq}=1.4\cdot10^{-9}$	**$Am(OH)_3$(am)** $[Am]_{aq}=9.8\cdot10^{-10}$	**$Am(OH)_3$(am)** $[Am]_{aq}=1.6\cdot10^{-9}$	**No precipitation** $[Am]_{aq}=1.1\cdot10^{-7}$
	$Am(OH)_3(ISAH_2)^-$ (63.0%) $Am(OH)_3$ (34.7%)	$Am(OH)_3$ (50.3%) $Am(OH)_3(ISAH_2)^-$ (45.6%)	$Am(OH)_3(ISAH_2)^-$ (56.3%) $Am(OH)_3$ (32.1%) $Am(OH)_2^+$ (11.5%)	$Am(EDTA)^-$ (53.8%) $Am(CO_3)^+$ (30.4%)
Pu $[Pu]_T=6.5\cdot10^{-9}$ ***PuO_2(coll, hyd) is never oversaturated***	**$Pu(OH)_4$(am)** $[Pu]_{aq}=3.6\cdot10^{-9}$	**$Pu(OH)_4$(am)** $[Pu]_{aq}=1.6\cdot10^{-9}$	**$Pu(OH)_4$(am)** $[Pu]_{aq}=3.1\cdot10^{-9}$	**$Pu(OH)_4$(am)** $[Pu]_{aq}=3.5\cdot10^{-9}$
	$Pu(OH)_4(ISAH_2)_2^{2-}$ (47.5%) $Pu(OH)_4(ISAH_2)^-$ (39.0%) $Pu(OH)_4$ (13.5%)	$Pu(OH)_4(ISAH_2)^-$ (44.7%) $Pu(OH)_4$ (31.1%) $Pu(OH)_4(ISAH_2)_2^{2-}$ (24.2%)	$Pu(OH)_4(ISAH_2)^-$ (44.4%) $Pu(OH)_4(ISAH_2)_2^{2-}$ (39.6%) $Pu(OH)_4$ (16.0%)	$Pu(OH)_4(ISAH_2)^-$ (43.5%) $Pu(OH)_4(ISAH_2)_2^{2-}$ (39.9%) $Pu(OH)_4$ (14.4%)

Table A 4. Radionuclide speciation and equilibrium concentration for Am and Pu in the SILO in absence of organics. Only species with ≥10% are shown.

Porewater	A	B	C	D
pH	13.06	12.60	11.60	9.66
pe	0	0	0	0
$[Ca]_T$ (M)	$1.49\cdot10^{-3}$	$2.00\cdot10^{-2}$	$2.59\cdot10^{-3}$	$4.57\cdot10^{-5}$
Am $[Am]_T = 1.1\cdot10^{-7}$	**$Am(OH)_3$(coll)** $[Am]_{aq} = 5.2\cdot10^{-9}$	**$Am(OH)_3$(coll)** $[Am]_{aq} = 5.4\cdot10^{-9}$	**$Am(OH)_3$(coll)** $[Am]_{aq} = 6.8\cdot10^{-9}$	**No precipitation** $[Am]_{aq} = 1.1\cdot10^{-7}$
	$Am(OH)_3$ (93.9%)	$Am(OH)_3$ (92.5%)	$Am(OH)_3$ (73.4%) $Am(OH)_2^+$ (26.4%)	$Am(CO_3)_2^-$ (66.5%) $Am(OH)_2^+$ (16.8%) $Am(CO_3)^+$ (10.3%)
	$Am(OH)_3$(am) $[Am]_{aq} = 5.2\cdot10^{-10}$	**$Am(OH)_3$(am)** $[Am]_{aq} = 5.4\cdot10^{-10}$	**$Am(OH)_3$(am)** $[Am]_{aq} = 6.8\cdot10^{-10}$	**$Am(OH)_3$(am)** $[Am]_{aq} = 9.0\cdot10^{-8}$
	$Am(OH)_3$ (93.9%)	$Am(OH)_3$ (92.5%)	$Am(OH)_3$ (73.4%) $Am(OH)_2^+$ (26.4%)	$Am(CO_3)_2^-$ (66.5%) $Am(OH)_2^+$ (16.8%) $Am(CO_3)^+$ (10.3%)
Pu $[Pu]_T = 6.5\cdot10^{-9}$	**PuO_2(coll, hyd)** $[Pu]_{aq} = 4.8\cdot10^{-9}$	**PuO_2(coll, hyd)** $[Pu]_{aq} = 4.9\cdot10^{-9}$	**PuO_2(coll, hyd)** $[Pu]_{aq} = 5.0\cdot10^{-9}$	**PuO_2(coll, hyd)** $[Pu]_{aq} = 5.1\cdot10^{-9}$
	$Pu(OH)_4$ (100%)	$Pu(OH)_4$ (100%)	$Pu(OH)_4$ (100%)	$Pu(OH)_4$ (97.9%)
	$Pu(OH)_4$(am) $[Pu]_{aq} = 4.8\cdot10^{-10}$	**$Pu(OH)_4$(am)** $[Pu]_{aq} = 4.9\cdot10^{-10}$	**$Pu(OH)_4$(am)** $[Pu]_{aq} = 5.0\cdot10^{-10}$	**$Pu(OH)_4$(am)** $[Pu]_{aq} = 5.1\cdot10^{-10}$
	$Pu(OH)_4$ (100%)	$Pu(OH)_4$ (100%)	$Pu(OH)_4$ (100%)	$Pu(OH)_4$ (97.9%)

Table A 5. Radionuclide speciation and equilibrium concentration for Am and Pu in the 1BMA. $[ISA]_{aq}=2.9\cdot10^{-4}$ M (considering ISA sorption). Only species accounting for ≥10% of the dissolved radionuclide speciation are shown.

Porewater	A	B	C	D
pH	13.06	12.60	11.60	9.66
pe	0	0	0	0
$[Ca]_T$ (M)	$1.48\cdot10^{-3}$	$2.00\cdot10^{-2}$	$2.59\cdot10^{-3}$	$4.57\cdot10^{-5}$
Am $[Am]_T=1.4\cdot10^{-10}$	**No precipitation** $[Am]_{aq}=1.4\cdot10^{-10}$	**No precipitation** $[Am]_{aq}=1.4\cdot10^{-10}$	**No precipitation** $[Am]_{aq}=1.4\cdot10^{-10}$	**No precipitation** $[Am]_{aq}=1.4\cdot10^{-10}$
	$Am(OH)_3(ISAH_2)^-$ (92.9%)	$Am(OH)_3(ISAH_2)^-$ (86.5%) $Am(OH)_3$ (12.5%)	$Am(OH)_3(ISAH_2)^-$ (90.8%)	$Am(CO_3)_2^-$ (61.5%) $Am(OH)_2^+$ (15.6%)
Pu $[Pu]_T=1.7\cdot10^{-9}$	**No precipitation** $[Pu]_{aq}=1.7\cdot10^{-9}$	**No precipitation** $[Pu]_{aq}=1.7\cdot10^{-9}$	**No precipitation** $[Pu]_{aq}=1.7\cdot10^{-9}$	**No precipitation** $[Pu]_{aq}=1.7\cdot10^{-9}$
	$Pu(OH)_4(ISAH_2)_2^{2-}$ (89.9%)	$Pu(OH)_4(ISAH_2)_2^{2-}$ (79.1%) $Pu(OH)_4(ISAH_2)^-$ (19.1%)	$Pu(OH)_4(ISAH_2)_2^{2-}$ (86.7%) $Pu(OH)_4(ISAH_2)^-$ (12.7%)	$Pu(OH)_4(ISAH_2)_2^{2-}$ (86.6%) $Pu(OH)_4(ISAH_2)^-$ (12.3%)

Table A 6. Radionuclide speciation and equilibrium concentration for Am and Pu in the 1BMA. $[EDTA]_T=3.8\cdot10^{-6}$ M. Only species with ≥10% are shown.

Porewater	A	B	C	D
pH	13.06	12.60	11.60	9.66
pe	0	0	0	0
$[Ca]_T$ (M)	$1.48\cdot10^{-3}$	$2.00\cdot10^{-2}$	$2.59\cdot10^{-3}$	$4.57\cdot10^{-5}$
Am $[Am]_T=1.4\cdot10^{-10}$	**No precipitation** $[Am]_{aq}=1.4\cdot10^{-10}$	**No precipitation** $[Am]_{aq}=1.4\cdot10^{-10}$	**No precipitation** $[Am]_{aq}=1.4\cdot10^{-10}$	**No precipitation** $[Am]_{aq}=1.4\cdot10^{-10}$
	$Am(OH)_3$ (93.9%)	$Am(OH)_3$ (92.5%)	$Am(OH)_3$ (73.4%) $Am(OH)_2^+$ (26.4%)	$Am(EDTA)^-$ (91.2%)
Pu $[Pu]_T=1.7\cdot10^{-9}$ ***PuO_2(coll, hyd) is never oversaturated***	**$Pu(OH)_4$(am)** $[Pu]_{aq}=4.8\cdot10^{-10}$	**$Pu(OH)_4$(am)** $[Pu]_{aq}=4.9\cdot10^{-10}$	**$Pu(OH)_4$(am)** $[Pu]_{aq}=5.0\cdot10^{-10}$	**$Pu(OH)_4$(am)** $[Pu]_{aq}=5.1\cdot10^{-10}$
	$Pu(OH)_4$ (100%)	$Pu(OH)_4$ (100%)	$Pu(OH)_4$ (100%)	$Pu(OH)_4$ (97.9%)

Table A 7. Radionuclide speciation and equilibrium concentration for Am and Pu in the 1BMA. $[ISA]_{aq}=2.9\cdot10^{-4}$ M (considering ISA sorption), $[EDTA]_T=3.8\cdot10^{-6}$ M. Only species accounting for ≥10% of the dissolved radionuclide speciation are shown.

Porewater	A	B	C	D
pH	13.06	12.60	11.60	9.66
pe	0	0	0	0
$[Ca]_T$ (M)	$1.48\cdot10^{-3}$	$2.00\cdot10^{-2}$	$2.59\cdot10^{-3}$	$4.57\cdot10^{-5}$
Am $[Am]_T=1.4\cdot10^{-10}$	**No precipitation** $[Am]_{aq}=1.4\cdot10^{-10}$	**No precipitation** $[Am]_{aq}=1.4\cdot10^{-10}$	**No precipitation** $[Am]_{aq}=1.4\cdot10^{-10}$	**No precipitation** $[Am]_{aq}=1.4\cdot10^{-10}$
	$Am(OH)_3(ISAH_2)^-$ (92.9%)	$Am(OH)_3(ISAH_2)^-$ (86.5%) $Am(OH)_3$ (12.5%)	$Am(OH)_3(ISAH_2)^-$ (90.8%)	$Am(EDTA)^-$ (90.7%)
Pu $[Pu]_T=1.7\cdot10^{-9}$	**No precipitation** $[Pu]_{aq}=1.7\cdot10^{-9}$	**No precipitation** $[Pu]_{aq}=1.7\cdot10^{-9}$	**No precipitation** $[Pu]_{aq}=1.7\cdot10^{-9}$	**No precipitation** $[Pu]_{aq}=1.7\cdot10^{-9}$
	$Pu(OH)_4(ISAH_2)_2^{2-}$ (89.9%)	$Pu(OH)_4(ISAH_2)_2^{2-}$ (79.1%) $Pu(OH)_4(ISAH_2)^-$ (19.1%)	$Pu(OH)_4(ISAH_2)_2^{2-}$ (86.7%) $Pu(OH)_4(ISAH_2)^-$ (12.7%)	$Pu(OH)_4(ISAH_2)_2^{2-}$ (86.6%) $Pu(OH)_4(ISAH_2)^-$ (12.3%)

Table A 8. Radionuclide speciation and equilibrium concentration for Am and Pu in the 1BMA in absence of organics. Only species with ≥10% are shown.

Porewater	A	B	C	D
pH	13.06	12.60	11.60	9.66
pe	0	0	0	0
$[Ca]_T$ (M)	$1.48\cdot10^{-3}$	$2.00\cdot10^{-2}$	$2.59\cdot10^{-3}$	$4.57\cdot10^{-5}$
Am $[Am]_T = 1.4\cdot10^{-10}$	**No precipitation** $[Am]_{aq} = 1.4\cdot10^{-10}$	**No precipitation** $[Am]_{aq} = 1.4\cdot10^{-10}$	**No precipitation** $[Am]_{aq} = 1.4\cdot10^{-10}$	**No precipitation** $[Am]_{aq} = 1.4\cdot10^{-10}$
	$Am(OH)_3$ (93.9%)	$Am(OH)_3$ (92.5%)	$Am(OH)_3$ (73.4%) $Am(OH)_2^+$ (26.4%)	$Am(CO_3)_2^-$ (66.5%) $Am(OH)_2^+$ (16.8%) $Am(CO_3)^+$ (10.3%)
Pu $[Pu]_T = 1.7\cdot10^{-9}$ ***PuO_2(coll, hyd) is never oversaturated***	**$Pu(OH)_4$(am)** $[Pu]_{aq} = 4.8\cdot10^{-10}$	**$Pu(OH)_4$(am)** $[Pu]_{aq} = 4.9\cdot10^{-10}$	**$Pu(OH)_4$(am)** $[Pu]_{aq} = 5.0\cdot10^{-10}$	**$Pu(OH)_4$(am)** $[Pu]_{aq} = 5.1\cdot10^{-10}$
	$Pu(OH)_4$ (100%)	$Pu(OH)_4$ (100%)	$Pu(OH)_4$ (100%)	$Pu(OH)_4$ (97.9%)

Table A 9. Radionuclide speciation and equilibrium concentration for Am and Pu in the 2BMA. $[ISA]_{aq}$=2.6·10-4 M (considering ISA sorption). Only species accounting for ≥10% of the dissolved radionuclide speciation are shown.

Porewater	A	B	C	D
pH	13.06	12.60	11.60	9.66
pe	0	0	0	0
$[Ca]_T$ (M)	$1.48\cdot10^{-3}$	$2.00\cdot10^{-2}$	$2.59\cdot10^{-3}$	$4.57\cdot10^{-5}$
Am $[Am]_T = 2.0\cdot10^{-10}$	**No precipitation** $[Am]_{aq} = 2.0\cdot10^{-10}$	**No precipitation** $[Am]_{aq} = 2.0\cdot10^{-10}$	**No precipitation** $[Am]_{aq} = 2.0\cdot10^{-10}$	**No precipitation** $[Am]_{aq} = 2.0\cdot10^{-10}$
	$Am(OH)_3(ISAH_2)^-$ (92.1%)	$Am(OH)_3(ISAH_2)^-$ (85.2%) $Am(OH)_3$ (13.7%)	$Am(OH)_3(ISAH_2)^-$ (89.9%)	$Am(CO_3)_2^-$ (62.0%) $Am(OH)_2^+$ (15.7%)
Pu $[Pu]_T = 2.2\cdot10^{-9}$	**No precipitation** $[Pu]_{aq} = 2.2\cdot10^{-9}$	**No precipitation** $[Pu]_{aq} = 2.2\cdot10^{-9}$	**No precipitation** $[Pu]_{aq} = 2.2\cdot10^{-9}$	**No precipitation** $[Pu]_{aq} = 2.2\cdot10^{-9}$
	$Pu(OH)_4(ISAH_2)_2^{2-}$ (88.8%) $Pu(OH)_4(ISAH_2)^-$ (10.6%)	$Pu(OH)_4(ISAH_2)_2^{2-}$ (77.1%) $Pu(OH)_4(ISAH_2)^-$ (20.8%)	$Pu(OH)_4(ISAH_2)_2^{2-}$ (85.3%) $Pu(OH)_4(ISAH_2)^-$ (13.9%)	$Pu(OH)_4(ISAH_2)_2^{2-}$ (85.2%) $Pu(OH)_4(ISAH_2)^-$ (13.5%)

Table A 10. Radionuclide speciation and equilibrium concentration for Am and Pu in the 2BMA in absence of organics. Only species with ≥10% are shown.

Porewater	A	B	C	D
pH	13.06	12.60	11.60	9.66
pe	0	0	0	0
$[Ca]_T$ (M)	$1.48 \cdot 10^{-3}$	$2.00 \cdot 10^{-2}$	$2.59 \cdot 10^{-3}$	$4.57 \cdot 10^{-5}$
Am $[Am]_T = 2.0 \cdot 10^{-10}$	**No precipitation** $[Am]_{aq} = 2.0 \cdot 10^{-10}$	**No precipitation** $[Am]_{aq} = 2.0 \cdot 10^{-10}$	**No precipitation** $[Am]_{aq} = 2.0 \cdot 10^{-10}$	**No precipitation** $[Am]_{aq} = 2.0 \cdot 10^{-10}$
	$Am(OH)_3$ (93.9%)	$Am(OH)_3$ (92.5%)	$Am(OH)_3$ (73.4%) $Am(OH)_2^+$ (26.4%)	$Am(CO_3)_2^-$ (66.5%) $Am(OH)_2^+$ (16.8%) $Am(CO_3)^+$ (10.3%)
Pu $[Pu]_T = 2.2 \cdot 10^{-9}$ ***PuO_2(coll, hyd) is never oversaturated***	**$Pu(OH)_4$(am)** $[Pu]_{aq} = 4.8 \cdot 10^{-10}$	**$Pu(OH)_4$(am)** $[Pu]_{aq} = 4.9 \cdot 10^{-10}$	**$Pu(OH)_4$(am)** $[Pu]_{aq} = 5.0 \cdot 10^{-10}$	**$Pu(OH)_4$(am)** $[Pu]_{aq} = 5.1 \cdot 10^{-10}$
	$Pu(OH)_4$ (100%)	$Pu(OH)_4$ (100%)	$Pu(OH)_4$ (100%)	$Pu(OH)_4$ (97.9%)

Table A 11. Radionuclide speciation and equilibrium concentration for Am and Pu in the BTF. $[ISA]_{aq}=4.5\cdot10^{-6}$ M (considering ISA sorption). Only species accounting for ≥10% of the dissolved radionuclide speciation are shown.

Porewater	A	B	C	D
pH	13.06	12.60	11.60	9.66
pe	0	0	0	0
$[Ca]_T$ (M)	$1.48\cdot10^{-3}$	$2.00\cdot10^{-2}$	$2.59\cdot10^{-3}$	$4.57\cdot10^{-5}$
Am $[Am]_T=2.0\cdot10^{-11}$	**No precipitation** $[Am]_{aq}=2.0\cdot10^{-11}$	**No precipitation** $[Am]_{aq}=2.0\cdot10^{-11}$	**No precipitation** $[Am]_{aq}=2.0\cdot10^{-11}$	**No precipitation** $[Am]_{aq}=2.0\cdot10^{-11}$
	$Am(OH)_3$ (78.1%) $Am(OH)_3(ISAH_2)^-$ (16.8%)	$Am(OH)_3$ (84.1%)	$Am(OH)_3$ (63.7%) $Am(OH)_2^+$ (22.9%)	$Am(CO_3)_2^-$ (66.5%) $Am(OH)_2^+$ (16.8%) $Am(CO_3)^+$ (10.3%)
Pu $[Pu]_T=2.6\cdot10^{-10}$	**No precipitation** $[Pu]_{aq}=2.6\cdot10^{-10}$	**No precipitation** $[Pu]_{aq}=2.6\cdot10^{-10}$	**No precipitation** $[Pu]_{aq}=2.6\cdot10^{-10}$	**No precipitation** $[Pu]_{aq}=2.6\cdot10^{-10}$
	$Pu(OH)_4$ (71.9%) $Pu(OH)_4(ISAH_2)^-$ (24.5%)	$Pu(OH)_4$ (84.7%) $Pu(OH)_4(ISAH_2)^-$ (14.4%)	$Pu(OH)_4$ (73.3%) $Pu(OH)_4(ISAH_2)^-$ (24.1%)	$Pu(OH)_4$ (69.7%) $Pu(OH)_4(ISAH_2)^-$ (25.0%)

Table A 12. Radionuclide speciation and equilibrium concentration for Am and Pu in the BTF. $[EDTA]_T=1.3\cdot10^{-6}$ M. Only species with ≥10% are shown.

Porewater	A	B	C	D
pH	13.06	12.60	11.60	9.66
pe	0	0	0	0
$[Ca]_T$ (M)	$1.48\cdot10^{-3}$	$2.00\cdot10^{-2}$	$2.59\cdot10^{-3}$	$4.57\cdot10^{-5}$
Am $[Am]_T=2.0\cdot10^{-11}$	**No precipitation** $[Am]_{aq}=2.0\cdot10^{-11}$	**No precipitation** $[Am]_{aq}=2.0\cdot10^{-11}$	**No precipitation** $[Am]_{aq}=2.0\cdot10^{-11}$	**No precipitation** $[Am]_{aq}=2.0\cdot10^{-11}$
	$Am(OH)_3$ (93.9%)	$Am(OH)_3$ (92.5%)	$Am(OH)_3$ (73.4%) $Am(OH)_2^+$ (26.4%)	$Am(EDTA)^-$ (77.1%) $Am(CO_3)_2^-$ (15.3%)
Pu $[Pu]_T=2.6\cdot10^{-10}$	**No precipitation** $[Pu]_{aq}=2.6\cdot10^{-10}$	**No precipitation** $[Pu]_{aq}=2.6\cdot10^{-10}$	**No precipitation** $[Pu]_{aq}=2.6\cdot10^{-10}$	**No precipitation** $[Pu]_{aq}=2.6\cdot10^{-10}$
	$Pu(OH)_4$ (100%)	$Pu(OH)_4$ (100%)	$Pu(OH)_4$ (100%)	$Pu(OH)_4$ (97.9%)

Table A 13. Radionuclide speciation and equilibrium concentration for Am and Pu in the BTF. $[ISA]_{aq}=4.5\cdot10^{-6}$ M (considering ISA sorption), $[EDTA]_T=1.3\cdot10^{-6}$ M. Only species accounting for ≥10% of the dissolved radionuclide speciation are shown.

Porewater	A	B	C	D
pH	13.06	12.60	11.60	9.66
pe	0	0	0	0
$[Ca]_T$ (M)	$1.48\cdot10^{-3}$	$2.00\cdot10^{-2}$	$2.59\cdot10^{-3}$	$4.57\cdot10^{-5}$
Am $[Am]_T=2.0\cdot10^{-11}$	**No precipitation** $[Am]_{aq}=2.0\cdot10^{-11}$	**No precipitation** $[Am]_{aq}=2.0\cdot10^{-11}$	**No precipitation** $[Am]_{aq}=2.0\cdot10^{-11}$	**No precipitation** $[Am]_{aq}=2.0\cdot10^{-11}$
	$Am(OH)_3$ (78.1%) $Am(OH)_3(ISAH_2)^-$ (16.8%)	$Am(OH)_3$ (84.1%)	$Am(OH)_3$ (63.7%) $Am(OH)_2^+$ (22.9%) $Am(OH)_3(ISAH_2)^-$ (13.2%)	$Am(EDTA)^-$ (77.1%) $Am(CO_3)_2^-$ (15.3%)
Pu $[Pu]_T=2.6\cdot10^{-10}$	**No precipitation** $[Pu]_{aq}=2.6\cdot10^{-10}$	**No precipitation** $[Pu]_{aq}=2.6\cdot10^{-10}$	**No precipitation** $[Pu]_{aq}=2.6\cdot10^{-10}$	**No precipitation** $[Pu]_{aq}=2.6\cdot10^{-10}$
	$Pu(OH)_4$ (71.9%) $Pu(OH)_4(ISAH_2)^-$ (24.5%)	$Pu(OH)_4$ (84.7%) $Pu(OH)_4(ISAH_2)^-$ (14.4%)	$Pu(OH)_4$ (73.3%) $Pu(OH)_4(ISAH_2)^-$ (24.1%)	$Pu(OH)_4$ (69.7%) $Pu(OH)_4(ISAH_2)^-$ (25.0%)

Table A 14. Radionuclide speciation and equilibrium concentration for Am and Pu in the BTF in absence of organics. Only species with ≥10% are shown.

Porewater	A	B	C	D
pH	13.06	12.60	11.60	9.66
pe	0	0	0	0
$[Ca]_T$ (M)	$1.48 \cdot 10^{-3}$	$2.00 \cdot 10^{-2}$	$2.59 \cdot 10^{-3}$	$4.57 \cdot 10^{-5}$
Am $[Am]_T = 2.0 \cdot 10^{-11}$	**No precipitation** $[Am]_{aq} = 2.0 \cdot 10^{-11}$	**No precipitation** $[Am]_{aq} = 2.0 \cdot 10^{-11}$	**No precipitation** $[Am]_{aq} = 2.0 \cdot 10^{-11}$	**No precipitation** $[Am]_{aq} = 2.0 \cdot 10^{-11}$
	$Am(OH)_3$ (93.9%)	$Am(OH)_3$ (92.5%)	$Am(OH)_3$ (73.4%) $Am(OH)_2^+$ (26.4%)	$Am(CO_3)_2^-$ (66.5%) $Am(OH)_2^+$ (16.8%) $Am(CO_3)^+$ (10.3%)
Pu $[Pu]_T = 2.6 \cdot 10^{-10}$	**No precipitation** $[Pu]_{aq} = 2.6 \cdot 10^{-10}$	**No precipitation** $[Pu]_{aq} = 2.6 \cdot 10^{-10}$	**No precipitation** $[Pu]_{aq} = 2.6 \cdot 10^{-10}$	**No precipitation** $[Pu]_{aq} = 2.6 \cdot 10^{-10}$
	$Pu(OH)_4$ (100%)	$Pu(OH)_4$ (100%)	$Pu(OH)_4$ (100%)	$Pu(OH)_4$ (97.9%)

Table A 15. Radionuclide speciation and equilibrium concentration for Am and Pu in the SILO. $[ISA]_{aq}=3.8\cdot10^{-5}$ M (considering ISA sorption). Only species accounting for ≥10% of the dissolved radionuclide speciation are shown.

Porewater	A	B	C	D
pH	13.06	12.60	11.60	9.66
pe	-11.79	-11.34	-10.35	-8.45
$[Ca]_T$ (M)	$1.49\cdot10^{-3}$	$2.00\cdot10^{-2}$	$2.59\cdot10^{-3}$	$4.57\cdot10^{-5}$
Am $[Am]_T=1.1\cdot10^{-7}$	**$Am(OH)_3$(coll)** $[Am]_{aq}=1.4\cdot10^{-8}$	**$Am(OH)_3$(coll)** $[Am]_{aq}=9.8\cdot10^{-9}$	**$Am(OH)_3$(coll)** $[Am]_{aq}=1.6\cdot10^{-8}$	**No precipitation** $[Am]_{aq}=1.1\cdot10^{-7}$
	$Am(OH)_3(ISAH_2)^-$ (63.0%) $Am(OH)_3$ (34.7%)	$Am(OH)_3$ (50.3%) $Am(OH)_3(ISAH_2)^-$ (45.6%)	$Am(OH)_3(ISAH_2)^-$ (56.3%) $Am(OH)_3$ (32.1%) $Am(OH)_2^+$ (11.5%)	$Am(CO_3)_2^-$ (65.8%) $Am(OH)_2^+$ (16.6%) $Am(CO_3)^+$ (10.2%)
	$Am(OH)_3$(am) $[Am]_{aq}=1.4\cdot10^{-9}$	**$Am(OH)_3$(am)** $[Am]_{aq}=9.8\cdot10^{-10}$	**$Am(OH)_3$(am)** $[Am]_{aq}=1.6\cdot10^{-9}$	**No precipitation** $[Am]_{aq}=9.1\cdot10^{-8}$
	$Am(OH)_3(ISAH_2)^-$ (63.1%) $Am(OH)_3$ (34.7%)	$Am(OH)_3$ (50.3%) $Am(OH)_3(ISAH_2)^-$ (45.6%)	$Am(OH)_3(ISAH_2)^-$ (56.3%) $Am(OH)_3$ (32.1%) $Am(OH)_2^+$ (11.5%)	$Am(CO_3)_2^-$ (65.8%) $Am(OH)_2^+$ (16.6%) $Am(CO_3)^+$ (10.2%)
Pu $[Pu]_T=6.5\cdot10^{-9}$ ***$Pu(OH)_3$(coll) is never oversaturated***	**$Pu(OH)_3$(cr)** $[Pu]_{aq}=5.7\cdot10^{-9}$	**$Pu(OH)_3$(cr)** $[Pu]_{aq}=2.7\cdot10^{-9}$	**$Pu(OH)_3$(cr)** $[Pu]_{aq}=4.8\cdot10^{-9}$	**No precipitation** $[Pu]_{aq}=6.5\cdot10^{-9}$
	$Pu(OH)_4(ISAH_2)_2^{2-}$ (45.0%) $Pu(OH)_4(ISAH_2)^-$ (36.9%) $Pu(OH)_4$ (12.8%)	$Pu(OH)_4(ISAH_2)^-$ (39.5%) $Pu(OH)_4$ (27.5%) $Pu(OH)_4(ISAH_2)_2^{2-}$ (21.3%) $Pu(OH)_3$ (11.7%)	$Pu(OH)_4(ISAH_2)^-$ (41.5%) $Pu(OH)_4(ISAH_2)_2^{2-}$ (37%) $Pu(OH)_4$ (14.9%)	$Pu(CO_3)_3^{3-}$ (46.3%) $Pu(CO_3)_2^-$ (23.0%) $Pu(OH)_4(ISAH_2)^-$ (11.0%) $Pu(OH)_4(ISAH_2)_2^{2-}$ (10.1%)

Table A 16. Radionuclide speciation and equilibrium concentration for Am and Pu in the SILO. $[EDTA]_{aq}=5.23\cdot10^{-7}$ M. Only species with ≥10% are shown.

Porewater	A	B	C	D
pH	13.06	12.60	11.60	9.66
pe	-11.79	-11.34	-10.35	-8.45
$[Ca]_T$ (M)	$1.49\cdot10^{-3}$	$2.00\cdot10^{-2}$	$2.59\cdot10^{-3}$	$4.57\cdot10^{-5}$
Am $[Am]_T=1.1\cdot10^{-7}$	**$Am(OH)_3$(coll)** $[Am]_{aq}=5.2\cdot10^{-9}$	**$Am(OH)_3$(coll)** $[Am]_{aq}=5.4\cdot10^{-9}$	**$Am(OH)_3$(coll)** $[Am]_{aq}=6.8\cdot10^{-9}$	**No precipitation** $[Am]_{aq}=1.1\cdot10^{-7}$
	$Am(OH)_3$ (93.9%)	$Am(OH)_3$ (92.5%)	$Am(OH)_3$ (73.4%) $Am(OH)_2^+$ (26.4%)	$Am(EDTA)^-$ (53.8%) $Am(CO_3)_2^-$ (30.7%)
Am $[Am]_T=1.1\cdot10^{-7}$	**$Am(OH)_3$(am)** $[Am]_{aq}=5.2\cdot10^{-10}$	**$Am(OH)_3$(am)** $[Am]_{aq}=5.4\cdot10^{-10}$	**$Am(OH)_3$(am)** $[Am]_{aq}=6.8\cdot10^{-10}$	**No precipitation** $[Am]_{aq}=1.1\cdot10^{-7}$
	$Am(OH)_3$ (93.9%)	$Am(OH)_3$ (92.5%)	$Am(OH)_3$ (73.4%) $Am(OH)_2^+$ (26.4%)	$Am(EDTA)^-$ (53.8%) $Am(CO_3)_2^-$ (30.7%)
Pu $[Pu]_T=6.5\cdot10^{-9}$ ***$Pu(OH)_3$(coll) is never oversaturated***	**$Pu(OH)_3$(cr)** $[Pu]_{aq}=1.0\cdot10^{-9}$	**$Pu(OH)_3$(cr)** $[Pu]_{aq}=1.0\cdot10^{-9}$	**$Pu(OH)_3$(cr)** $[Pu]_{aq}=1.0\cdot10^{-9}$	**No precipitation** $[Pu]_{aq}=6.5\cdot10^{-9}$
	$Pu(OH)_4$ (70.5%) $Pu(OH)_3$ (29.5%)	$Pu(OH)_4$ (70.1%) $Pu(OH)_3$ (29.9%)	$Pu(OH)_4$ (69.4%) $Pu(OH)_3$ (30.3%)	$Pu(EDTA)^-$ (65.7%) $Pu(CO_3)_3^{3-}$ (20.3%) $Pu(CO_3)_2^-$ (10.1%)

Table A 17. Radionuclide speciation and equilibrium concentration for Am and Pu in the SILO. $[ISA]_{aq}=3.8\cdot10^{-5}$ M (considering ISA sorption) and $[EDTA]_T=5.23\cdot10^{-7}$ M. Only species accounting for ≥10% of the dissolved radionuclide speciation are shown.

Porewater	A	B	C	D
pH	13.06	12.60	11.60	9.66
pe	-11.79	-11.34	-10.35	-8.45
$[Ca]_T$ (M)	$1.49\cdot10^{-3}$	$2.00\cdot10^{-2}$	$2.59\cdot10^{-3}$	$4.57\cdot10^{-5}$
Am $[Am]_T=1.1\cdot10^{-7}$	**$Am(OH)_3$(coll)** $[Am]_{aq}=1.4\cdot10^{-8}$	**$Am(OH)_3$(coll)** $[Am]_{aq}=9.8\cdot10^{-9}$	**$Am(OH)_3$(coll)** $[Am]_{aq}=1.6\cdot10^{-8}$	**No precipitation** $[Am]_{aq}=1.1\cdot10^{-7}$
	$Am(OH)_3(ISAH_2)^-$ (63.1%) $Am(OH)_3$ (34.7%)	$Am(OH)_3$ (50.3%) $Am(OH)_3(ISAH_2)^-$ (45.6%)	$Am(OH)_3(ISAH_2)^-$ (56.3%) $Am(OH)_3$ (32.1%) $Am(OH)_2^+$ (11.5%)	$Am((EDTA)^-$ (53.6%) $Am(CO_3)_2^-$ (30.5%)
	$Am(OH)_3$(am) $[Am]_{aq}=1.4\cdot10^{-9}$	**$Am(OH)_3$(am)** $[Am]_{aq}=9.8\cdot10^{-10}$	**$Am(OH)_3$(am)** $[Am]_{aq}=1.6\cdot10^{-9}$	**No precipitation** $[Am]_{aq}=1.1\cdot10^{-7}$
	$Am(OH)_3(ISAH_2)^-$ (63.1%) $Am(OH)_3$ (34.7%)	$Am(OH)_3$ (50.3%) $Am(OH)_3(ISAH_2)^-$ (45.6%)	$Am(OH)_3(ISAH_2)^-$ (56.3%) $Am(OH)_3$ (32.1%) $Am(OH)_2^+$ (11.5%)	$Am(EDTA)^-$ (53.6%) $Am(CO_3)_2^-$ (30.5%)
Pu $[Pu]_T=6.5\cdot10^{-9}$ ***$Pu(OH)_3$(coll) is never oversaturated***	**$Pu(OH)_3$(cr)** $[Pu]_{aq}=5.7\cdot10^{-9}$	**$Pu(OH)_3$(cr)** $[Pu]_{aq}=2.7\cdot10^{-9}$	**$Pu(OH)_3$(cr)** $[Pu]_{aq}=4.8\cdot10^{-9}$	**No precipitation** $[Pu]_{aq}=6.5\cdot10^{-9}$
	$Pu(OH)_4(ISAH_2)_2^{2-}$ (45.0%) $Pu(OH)_4(ISAH_2)^-$ (36.9%) $Pu(OH)_4$ (12.8%)	$Pu(OH)_4(ISAH_2)^-$ (39.5%) $Pu(OH)_4$ (27.5%) $Pu(OH)_4(ISAH_2)_2^{2-}$ (21.3%) $Pu(OH)_3$ (11.7%)	$Pu(OH)_4(ISAH_2)^-$ (41.5%) $Pu(OH)_4(ISAH_2)_2^{2-}$ (37%) $Pu(OH)_4$ (14.9%)	$Pu(EDTA)^-$ (60.0%) $Pu(CO_3)_3^{3-}$ (18.5%)

Table A 18. Radionuclide speciation and equilibrium concentration for Am and Pu in the SILO in absence of organics. Only species with ≥10% are shown.

Porewater	A	B	C	D
pH	13.06	12.60	11.60	9.66
pe	-11.79	-11.34	-10.35	-8.45
$[Ca]_T$ (M)	$1.49\cdot10^{-3}$	$2.00\cdot10^{-2}$	$2.59\cdot10^{-3}$	$4.57\cdot10^{-5}$
Am $[Am]_T = 1.1\cdot10^{-7}$	**$Am(OH)_3$(coll)** $[Am]_{aq} = 5.2\cdot10^{-9}$	**$Am(OH)_3$(coll)** $[Am]_{aq} = 5.4\cdot10^{-9}$	**$Am(OH)_3$(coll)** $[Am]_{aq} = 6.8\cdot10^{-9}$	**No precipitation** $[Am]_{aq} = 1.1\cdot10^{-7}$
	$Am(OH)_3$ (93.9%)	$Am(OH)_3$ (92.5%)	$Am(OH)_3$ (73.4%) $Am(OH)_2^+$ (26.4%)	$Am(CO_3)_2^-$ (66.5%) $Am(OH)_2^+$ (16.8%) $Am(CO_3)^+$ (10.3%)
	$Am(OH)_3$(am) $[Am]_{aq} = 5.2\cdot10^{-10}$	**$Am(OH)_3$(am)** $[Am]_{aq} = 5.4\cdot10^{-10}$	**$Am(OH)_3$(am)** $[Am]_{aq} = 6.8\cdot10^{-10}$	**$Am(OH)_3$(am)** $[Am]_{aq} = 9.0\cdot10^{-8}$
	$Am(OH)_3$ (93.9%)	$Am(OH)_3$ (92.5%)	$Am(OH)_3$ (73.4%) $Am(OH)_2^+$ (26.4%)	$Am(CO_3)_2^-$ (66.5%) $Am(OH)_2^+$ (16.8%) $Am(CO_3)^+$ (10.3%)
Pu $[Pu]_T = 6.5\cdot10^{-9}$ ***$Pu(OH)_3$(coll) is never oversaturated***	**$Pu(OH)_3$(cr)** $[Pu]_{aq} = 1.03\cdot10^{-9}$ $Pu(OH)_4$ (70.5%) $Pu(OH)_3$ (29.5%)	**$Pu(OH)_3$(cr)** $[Pu]_{aq} = 1.04\cdot10^{-9}$ $Pu(OH)_4$ (70.1%) $Pu(OH)_3$ (29.9%)	**$Pu(OH)_3$(cr)** $[Pu]_{aq} = 1.04\cdot10^{-9}$ $Pu(OH)_4$ (69.4%) $Pu(OH)_3$ (30.3%)	**No precipitation** $[Pu]_{aq} = 6.5\cdot10^{-9}$ $Pu(CO_3)_3^{3-}$ (59.0%) $Pu(CO_3)_2^-$ (29.4%)

Table A 19. Radionuclide speciation and equilibrium concentration for Am and Pu in the 1BMA. $[ISA]_{aq}=2.9\cdot10^{-4}$ M (considering ISA sorption). Only species accounting for ≥10% of the dissolved radionuclide speciation are shown.

Porewater	A	B	C	D
pH	13.06	12.60	11.60	9.66
pe	-11.79	-11.34	-10.35	-8.45
$[Ca]_T$ (M)	$1.48\cdot10^{-3}$	$2.00\cdot10^{-2}$	$2.59\cdot10^{-3}$	$4.57\cdot10^{-5}$
Am $[Am]_T=1.4\cdot10^{-10}$	**No precipitation** $[Am]_{aq}=1.4\cdot10^{-10}$	**No precipitation** $[Am]_{aq}=1.4\cdot10^{-10}$	**No precipitation** $[Am]_{aq}=1.4\cdot10^{-10}$	**No precipitation** $[Am]_{aq}=1.4\cdot10^{-10}$
	$Am(OH)_3(ISAH_2)^-$ (92.9%)	$Am(OH)_3(ISAH_2)^-$ (86.5%) $Am(OH)_3$ (12.5%)	$Am(OH)_3(ISAH_2)^-$ (90.8%)	$Am(CO_3)_2^-$ (61.5%) $Am(OH)_2^+$ (15.6%) $Am(CO_3)^+$ (9.6%)
Pu $[Pu]_T=1.7\cdot10^{-9}$	**No precipitation** $[Pu]_{aq}=1.7\cdot10^{-9}$	**No precipitation** $[Pu]_{aq}=1.7\cdot10^{-9}$	**No precipitation** $[Pu]_{aq}=1.7\cdot10^{-9}$	**No precipitation** $[Pu]_{aq}=1.7\cdot10^{-9}$
	$Pu(OH)_4(ISAH_2)_2^{2-}$ (89.8%)	$Pu(OH)_4(ISAH_2)_2^{2-}$ (78.5%) $Pu(OH)_4(ISAH_2)^-$ (19.0%)	$Pu(OH)_4(ISAH_2)_2^{2-}$ (86.5%) $Pu(OH)_4(ISAH_2)^-$ (12.7%)	$Pu(OH)_4(ISAH_2)_2^{2-}$ (78.0%) $Pu(OH)_4(ISAH_2)^-$ (11.1%)

Table A 20. Radionuclide speciation and equilibrium concentration for Am and Pu in the 1BMA. $[EDTA]_T=3.8\cdot10^{-6}$ M. Only species with ≥10% are shown.

Porewater	A	B	C	D
pH	13.06	12.60	11.60	9.66
pe	-11.79	-11.34	-10.35	-8.45
$[Ca]_T$ (M)	$1.48\cdot10^{-3}$	$2.00\cdot10^{-2}$	$2.59\cdot10^{-3}$	$4.57\cdot10^{-5}$
Am $[Am]_T=1.4\cdot10^{-10}$	**No precipitation** $[Am]_{aq}=1.4\cdot10^{-10}$	**No precipitation** $[Am]_{aq}=1.4\cdot10^{-10}$	**No precipitation** $[Am]_{aq}=1.4\cdot10^{-10}$	**No precipitation** $[Am]_{aq}=1.4\cdot10^{-10}$
	$Am(OH)_3$ (93.9%)	$Am(OH)_3$ (92.5%)	$Am(OH)_3$ (73.4%) $Am(OH)_2^+$ (26.4%)	$Am(EDTA)^-$ (91.2%)
Pu $[Pu]_T=1.7\cdot10^{-9}$	**$Pu(OH)_3$(cr)** $[Pu]_{aq}=1.0\cdot10^{-9}$	**$Pu(OH)_3$(cr)** $[Pu]_{aq}=1.0\cdot10^{-9}$	**$Pu(OH)_3$(cr)** $[Pu]_{aq}=1.0\cdot10^{-9}$	**No precipitation** $[Pu]_{aq}=1.7\cdot10^{-9}$
	$Pu(OH)_4$ (70.5%) $Pu(OH)_3$ (29.5%)	$Pu(OH)_4$ (70.1%) $Pu(OH)_3$ (29.9%)	$Pu(OH)_4$ (69.4%) $Pu(OH)_3$ (30.3%)	$Pu(EDTA)^-$ (94.4%)

Table A 21. Radionuclide speciation and equilibrium concentration for Am and Pu in the 1BMA. $[ISA]_{aq}=2.9\cdot10^{-4}$ M (considering ISA sorption), $[EDTA]_T=3.8\cdot10^{-6}$ M. Only species accounting for ≥10% of the dissolved radionuclide speciation are shown.

Porewater	A	B	C	D
pH	13.06	12.60	11.60	9.66
pe	-11.79	-11.34	-10.35	-8.45
$[Ca]_T$ (M)	$1.48\cdot10^{-3}$	$2.00\cdot10^{-2}$	$2.59\cdot10^{-3}$	$4.57\cdot10^{-5}$
Am $[Am]_T=1.4\cdot10^{-10}$	**No precipitation** $[Am]_{aq}=1.4\cdot10^{-10}$	**No precipitation** $[Am]_{aq}=1.4\cdot10^{-10}$	**No precipitation** $[Am]_{aq}=1.4\cdot10^{-10}$	**No precipitation** $[Am]_{aq}=1.4\cdot10^{-10}$
	$Am(OH)_3(ISAH_2)^-$ (92.9%)	$Am(OH)_3(ISAH_2)^-$ (86.5%) $Am(OH)_3$ (12.5%)	$Am(OH)_3(ISAH_2)^-$ (90.8%)	$Am(EDTA)^-$ (90.7%)
Pu $[Pu]_T=1.7\cdot10^{-9}$	**No precipitation** $[Pu]_{aq}=1.7\cdot10^{-9}$	**No precipitation** $[Pu]_{aq}=1.7\cdot10^{-9}$	**No precipitation** $[Pu]_{aq}=1.7\cdot10^{-9}$	**No precipitation** $[Pu]_{aq}=1.7\cdot10^{-9}$
	$Pu(OH)_4(ISAH_2)_2^{2-}$ (89.8%)	$Pu(OH)_4(ISAH_2)_2^{2-}$ (78.5%) $Pu(OH)_4(ISAH_2)^-$ (19.0%)	$Pu(OH)_4(ISAH_2)_2^{2-}$ (86.5%) $Pu(OH)_4(ISAH_2)^-$ (12.7%)	$Pu(EDTA)^-$ (64.0%) $Pu(OH)_4(ISAH_2)_2^{2-}$ (28.1%)

Table A 22. Radionuclide speciation and equilibrium concentration for Am and Pu in the 1BMA in absence of organics. Only species with ≥10% are shown.

Porewater	A	B	C	D
pH	13.06	12.60	11.60	9.66
pe	-11.79	-11.34	-10.35	-8.45
$[Ca]_T$ (M)	$1.48\cdot10^{-3}$	$2.00\cdot10^{-2}$	$2.59\cdot10^{-3}$	$4.57\cdot10^{-5}$
Am $[Am]_T = 1.4\cdot10^{-10}$	**No precipitation** $[Am]_{aq} = 1.4\cdot10^{-10}$	**No precipitation** $[Am]_{aq} = 1.4\cdot10^{-10}$	**No precipitation** $[Am]_{aq} = 1.4\cdot10^{-10}$	**No precipitation** $[Am]_{aq} = 1.4\cdot10^{-10}$
	$Am(OH)_3$ (93.9%)	$Am(OH)_3$ (92.5%)	$Am(OH)_3$ (73.4%) $Am(OH)_2^+$ (26.4%)	$Am(CO_3)_2^-$ (66.5%) $Am(OH)_2^+$ (16.8%) $Am(CO_3)^+$ (10.3%)
Pu $[Pu]_T = 1.7\cdot10^{-9}$ ***$Pu(OH)_3$(coll) is never oversaturated***	**$Pu(OH)_3$(cr)** $[Pu]_{aq} = 1.0\cdot10^{-9}$	**$Pu(OH)_3$(cr)** $[Pu]_{aq} = 1.0\cdot10^{-9}$	**$Pu(OH)_3$(cr)** $[Pu]_{aq} = 1.0\cdot10^{-9}$	**No precipitation** $[Pu]_{aq} = 1.7\cdot10^{-9}$
	$Pu(OH)_4$ (70.5%) $Pu(OH)_3$ (29.5%)	$Pu(OH)_4$ (70.1%) $Pu(OH)_3$ (29.9%)	$Pu(OH)_4$ (69.4%) $Pu(OH)_3$ (30.3%)	$Pu(CO_3)_3^{3-}$ (59.0%) $Pu(CO_3)_2^-$ (29.4%)

Table A 23. Radionuclide speciation and equilibrium concentration for Am and Pu in the 2BMA. $[ISA]_{aq}$=2.6·10-4 M (considering ISA sorption). Only species accounting for ≥10% of the dissolved radionuclide speciation are shown.

Porewater	A	B	C	D
pH	13.06	12.60	11.60	9.66
pe	-11.79	-11.34	-10.35	-8.45
$[Ca]_T$ (M)	$1.48\cdot10^{-3}$	$2.00\cdot10^{-2}$	$2.59\cdot10^{-3}$	$4.57\cdot10^{-5}$
Am $[Am]_T = 2.0\cdot10^{-10}$	**No precipitation** $[Am]_{aq} = 2.0\cdot10^{-10}$	**No precipitation** $[Am]_{aq} = 2.0\cdot10^{-10}$	**No precipitation** $[Am]_{aq} = 2.0\cdot10^{-10}$	**No precipitation** $[Am]_{aq} = 2.0\cdot10^{-10}$
	$Am(OH)_3(ISAH_2)^-$ (92.1%)	$Am(OH)_3(ISAH_2)^-$ (85.2%) $Am(OH)_3$ (13.7%)	$Am(OH)_3(ISAH_2)^-$ (89.8%)	$Am(CO_3)_2^-$ (62.0%) $Am(OH)_2^+$ (15.7%) $Am(CO_3)^+$ (9.6%)
Pu $[Pu]_T = 2.2\cdot10^{-9}$	**No precipitation** $[Pu]_{aq} = 2.2\cdot10^{-9}$	**No precipitation** $[Pu]_{aq} = 2.2\cdot10^{-9}$	**No precipitation** $[Pu]_{aq} = 2.2\cdot10^{-9}$	**No precipitation** $[Pu]_{aq} = 2.2\cdot10^{-9}$
	$Pu(OH)_4(ISAH_2)_2^{2-}$ (88.6%) $Pu(OH)_4(ISAH_2)^-$ (10.6%)	$Pu(OH)_4(ISAH_2)_2^{2-}$ (76.4%) $Pu(OH)_4(ISAH_2)^-$ (20.6%)	$Pu(OH)_4(ISAH_2)_2^{2-}$ (85.0%) $Pu(OH)_4(ISAH_2)^-$ (13.9%)	$Pu(OH)_4(ISAH_2)_2^{2-}$ (75.1%) $Pu(OH)_4(ISAH_2)^-$ (11.9%)

Table A 24. Radionuclide speciation and equilibrium concentration for Am and Pu in the 2BMA in absence of organics. Only species with ≥10% are shown.

Porewater	A	B	C	D
pH	13.06	12.60	11.60	9.66
pe	-11.79	-11.34	-10.35	-8.45
$[Ca]_T$ (M)	$1.48 \cdot 10^{-3}$	$2.00 \cdot 10^{-2}$	$2.59 \cdot 10^{-3}$	$4.57 \cdot 10^{-5}$
Am $[Am]_T = 2.0 \cdot 10^{-10}$	**No precipitation** $[Am]_{aq} = 2.0 \cdot 10^{-10}$	**No precipitation** $[Am]_{aq} = 2.0 \cdot 10^{-10}$	**No precipitation** $[Am]_{aq} = 2.0 \cdot 10^{-10}$	**No precipitation** $[Am]_{aq} = 2.0 \cdot 10^{-10}$
	$Am(OH)_3$ (93.9%)	$Am(OH)_3$ (92.5%)	$Am(OH)_3$ (73.4%) $Am(OH)_2^+$ (26.4%)	$Am(CO_3)_2^-$ (66.5%) $Am(OH)_2^+$ (16.8%) $Am(CO_3)^+$ (10.3%)
Pu $[Pu]_T = 2.2 \cdot 10^{-9}$ ***$Pu(OH)_3$(coll) is never oversaturated***	**$Pu(OH)_3$(cr)** $[Pu]_{aq} = 1.0 \cdot 10^{-9}$	**$Pu(OH)_3$(cr)** $[Pu]_{aq} = 1.0 \cdot 10^{-9}$	**$Pu(OH)_3$(cr)** $[Pu]_{aq} = 1.0 \cdot 10^{-9}$	**No precipitation** $[Pu]_{aq} = 2.2 \cdot 10^{-9}$
	$Pu(OH)_4$ (70.5%) $Pu(OH)_3$ (29.5%)	$Pu(OH)_4$ (70.1%) $Pu(OH)_3$ (29.9%)	$Pu(OH)_4$ (69.4%) $Pu(OH)_3$ (30.3%)	$Pu(CO_3)_3^{3-}$ (59.0%) $Pu(CO_2)_2^-$ (29.4%)

Table A 25. Radionuclide speciation and equilibrium concentration for Am and Pu in the BTF. $[ISA]_{aq}=4.5\cdot10^{-6}$ M (considering ISA sorption). Only species accounting for ≥10% of the dissolved radionuclide speciation are shown.

Porewater	A	B	C	D
pH	13.06	12.60	11.60	9.66
pe	-11.79	-11.34	-10.35	-8.45
$[Ca]_T$ (M)	$1.48\cdot10^{-3}$	$2.00\cdot10^{-2}$	$2.59\cdot10^{-3}$	$4.57\cdot10^{-5}$
Am $[Am]_T=2.0\cdot10^{-11}$	**No precipitation** $[Am]_{aq}=2.0\cdot10^{-11}$	**No precipitation** $[Am]_{aq}=2.0\cdot10^{-11}$	**No precipitation** $[Am]_{aq}=2.0\cdot10^{-11}$	**No precipitation** $[Am]_{aq}=2.0\cdot10^{-11}$
	$Am(OH)_3$ (78.1%) $Am(OH)_3(ISAH_2)^-$ (16.8%)	$Am(OH)_3$ (84.1%) $Am(OH)_3(ISAH_2)^-$ (9.0%)	$Am(OH)_3$ (63.7%) $Am(OH)_2^+$ (22.9%) $Am(OH)_3(ISAH_2)^-$ (13.2%)	$Am(CO_3)_2^-$ (66.5%) $Am(OH)_2^+$ (16.8%) $Am(CO_3)^+$ (10.3%)
Pu $[Pu]_T=2.6\cdot10^{-10}$	**No precipitation** $[Pu]_{aq}=2.6\cdot10^{-10}$	**No precipitation** $[Pu]_{aq}=2.6\cdot10^{-10}$	**No precipitation** $[Pu]_{aq}=2.6\cdot10^{-10}$	**No precipitation** $[Pu]_{aq}=2.6\cdot10^{-10}$
	$Pu(OH)_4$ (55.2%) $Pu(OH)_3$ (23.2%) $Pu(OH)_4(ISAH_2)^-$ (18.9%)	$Pu(OH)_4$ (62.2%) $Pu(OH)_3$ (26.6%) $Pu(OH)_4(ISAH_2)^-$ (10.6%)	$Pu(OH)_4$ (55.4%) $Pu(OH)_3$ (24.2%) $Pu(OH)_4(ISAH_2)^-$ (18.2%)	$Pu(CO_3)_3^{3-}$ (57.9%) $Pu(CO_3)_2^-$ (28.8%)

Table A 26. Radionuclide speciation and equilibrium concentration for Am and Pu in the BTF. $[EDTA]_T=1.3\cdot10^{-6}$ M. Only species with ≥10% are shown.

Porewater	A	B	C	D
pH	13.06	12.60	11.60	9.66
pe	-11.79	-11.34	-10.35	-8.45
$[Ca]_T$ (M)	$1.48\cdot10^{-3}$	$2.00\cdot10^{-2}$	$2.59\cdot10^{-3}$	$4.57\cdot10^{-5}$
Am $[Am]_T=2.0\cdot10^{-11}$	**No precipitation** $[Am]_{aq}=2.0\cdot10^{-11}$	**No precipitation** $[Am]_{aq}=2.0\cdot10^{-11}$	**No precipitation** $[Am]_{aq}=2.0\cdot10^{-11}$	**No precipitation** $[Am]_{aq}=2.0\cdot10^{-11}$
	$Am(OH)_3$ (93.9%)	$Am(OH)_3$ (92.5%)	$Am(OH)_3$ (73.4%) $Am(OH)_2^+$ (26.4%)	$Am(EDTA)^-$ (77.1%) $Am(CO_3)_2^-$ (15.3%)
Pu $[Pu]_T=2.6\cdot10^{-10}$	**No precipitation** $[Pu]_{aq}=2.6\cdot10^{-10}$	**No precipitation** $[Pu]_{aq}=2.6\cdot10^{-10}$	**No precipitation** $[Pu]_{aq}=2.6\cdot10^{-10}$	**No precipitation** $[Pu]_{aq}=2.6\cdot10^{-10}$
	$Pu(OH)_4$ (70.5%) $Pu(OH)_3$ (29.5%)	$Pu(OH)_4$ (70.1%) $Pu(OH)_3$ (29.9%)	$Pu(OH)_4$ (69.4%) $Pu(OH)_3$ (30.3%)	$Pu(EDTA)^-$ (84.6%) $Pu(CO_3)_3^{3-}$ (9.1%)

Table A 27. Radionuclide speciation and equilibrium concentration for Am and Pu in the BTF. $[ISA]_{aq}=4.5\cdot10^{-6}$ M (considering ISA sorption) and $[EDTA]_T=1.3\cdot10^{-6}$ M. Only species accounting for ≥10% of the dissolved radionuclide speciation are shown.

Porewater	A	B	C	D
pH	13.06	12.60	11.60	9.66
pe	-11.79	-11.34	-10.35	-8.45
$[Ca]_T$ (M)	$1.48\cdot10^{-3}$	$2.00\cdot10^{-2}$	$2.59\cdot10^{-3}$	$4.57\cdot10^{-5}$
Am $[Am]_T=2.0\cdot10^{-11}$	**No precipitation** $[Am]_{aq}=2.0\cdot10^{-11}$	**No precipitation** $[Am]_{aq}=2.0\cdot10^{-11}$	**No precipitation** $[Am]_{aq}=2.0\cdot10^{-11}$	**No precipitation** $[Am]_{aq}=2.0\cdot10^{-11}$
	$Am(OH)_3$ (78.1%) $Am(OH)_3(ISAH_2)^-$ (16.8%)	$Am(OH)_3$ (84.1%) $Am(OH)_3(ISAH_2)^-$ (9.0%)	$Am(OH)_3$ (63.7%) $Am(OH)_2^+$ (22.9%) $Am(OH)_3(ISAH_2)^-$ (13.2%)	$Am(EDTA)^-$ (77.1%) $Am(CO_3)_2^-$ (15.3%)
Pu $[Pu]_T=2.6\cdot10^{-10}$	**No precipitation** $[Pu]_{aq}=2.6\cdot10^{-10}$	**No precipitation** $[Pu]_{aq}=2.6\cdot10^{-10}$	**No precipitation** $[Pu]_{aq}=2.6\cdot10^{-10}$	**No precipitation** $[Pu]_{aq}=2.6\cdot10^{-10}$
	$Pu(OH)_4$ (55.2%) $Pu(OH)_3$ (23.2%) $Pu(OH)_4(ISAH_2)^-$ (18.9%)	$Pu(OH)_4$ (62.2%) $Pu(OH)_3$ (26.6%) $Pu(OH)_4(ISAH_2)^-$ (10.6%)	$Pu(OH)_4$ (55.4%) $Pu(OH)_3$ (24.2%) $Pu(OH)_4(ISAH_2)^-$ (18.2%)	$Pu(EDTA)^-$ (84.4%) $Pu(CO_3)_3^{3-}$ (9.0%)

Table A 28. Radionuclide speciation and equilibrium concentration for Am and Pu in the BTF. Only species with ≥10% are shown.

Porewater	A	B	C	D
pH	13.06	12.60	11.60	9.66
pe	-11.79	-11.34	-10.35	-8.45
$[Ca]_T$ (M)	$1.48 \cdot 10^{-3}$	$2.00 \cdot 10^{-2}$	$2.59 \cdot 10^{-3}$	$4.57 \cdot 10^{-5}$
Am $[Am]_T = 2.0 \cdot 10^{-11}$	**No precipitation** $[Am]_{aq} = 2.0 \cdot 10^{-11}$	**No precipitation** $[Am]_{aq} = 2.0 \cdot 10^{-11}$	**No precipitation** $[Am]_{aq} = 2.0 \cdot 10^{-11}$	**No precipitation** $[Am]_{aq} = 2.0 \cdot 10^{-11}$
	$Am(OH)_3$ (93.9%)	$Am(OH)_3$ (92.5%)	$Am(OH)_3$ (73.4%) $Am(OH)_2^+$ (26.4%)	$Am(CO_3)_2^-$ (66.5%) $Am(OH)_2^+$ (16.8%) $Am(CO_3)^+$ (10.3%)
Pu $[Pu]_T = 2.6 \cdot 10^{-10}$	**No precipitation** $[Pu]_{aq} = 2.6 \cdot 10^{-10}$	**No precipitation** $[Pu]_{aq} = 2.6 \cdot 10^{-10}$	**No precipitation** $[Pu]_{aq} = 2.6 \cdot 10^{-10}$	**No precipitation** $[Pu]_{aq} = 2.6 \cdot 10^{-10}$
	$Pu(OH)_4$ (70.5%) $Pu(OH)_3$ (29.5%)	$Pu(OH)_4$ (70.1%) $Pu(OH)_3$ (29.9%)	$Pu(OH)_4$ (69.4%) $Pu(OH)_3$ (30.3%)	$Pu(CO_3)_3^{3-}$ (59.0%) $Pu(CO_3)_2^-$ (29.4%)